Modeling of the Free Radical Copolymerization Kinetics of n-Butyl Acrylate, Methyl Methacrylate and 2-Ethylhexyl Acrylate Using PREDICI®

Authors:

Javier A. Gómez-Reguera, Eduardo Vivaldo-Lima, Vida A. Gabriel, Marc A. Dubé

Date Submitted: 2019-09-05

Keywords: Modelling, polymerization kinetics, n-butyl acrylate, methyl methacrylate, 2-ethylhexyl acrylate

Abstract:

Kinetic modeling of the bulk free radical copolymerizations of n-butyl acrylate (BA) and 2-ethylhexyl acrylate (EHA); methyl methacrylate (MMA) and EHA; as well as BA, MMA and EHA was performed using the software PREDICI®. Predicted results of conversion versus time, composition versus conversion, and molecular weight development are compared against experimental data at different feed compositions. Diffusion-controlled effects and backbiting for BA were incorporated into the model as they proved to be significant in these polymerizations. The set of estimated global parameters allows one to assess the performance of these copolymerization systems over a wide range of monomer compositions.

Record Type: Published Article

Submitted To: LAPSE (Living Archive for Process Systems Engineering)

Citation (overall record, always the latest version):	LAPSE:2019.0974
Citation (this specific file, latest version):	LAPSE:2019.0974-1
Citation (this specific file, this version):	LAPSE:2019.0974-1v1

DOI of Published Version: https://doi.org/10.3390/pr7070395

processes

MDPI

Article

Modeling of the Free Radical Copolymerization Kinetics of n-Butyl Acrylate, Methyl Methacrylate and 2-Ethylhexyl Acrylate Using PREDICI®

Javier A. Gómez-Reguera [1], Eduardo Vivaldo-Lima [1], Vida A. Gabriel [2] and Marc A. Dubé [2,*]

[1] Departamento de Ingeniería Química, Facultad de Química, Universidad Nacional Autónoma de México, 04510 Ciudad de México, Mexico

[2] Department of Chemical and Biological Engineering, Centre for Catalysis Research and Innovation, University of Ottawa, 161 Louis Pasteur Pvt., Ottawa, ON K1N 6N5, Canada

* Correspondence: marc.dube@uottawa.ca; Tel.: +1-613-562-5915; Fax: +1-613-562-5174

Received: 30 April 2019; Accepted: 19 June 2019; Published: 26 June 2019

Abstract: Kinetic modeling of the bulk free radical copolymerizations of n-butyl acrylate (BA) and 2-ethylhexyl acrylate (EHA); methyl methacrylate (MMA) and EHA; as well as BA, MMA and EHA was performed using the software PREDICI®. Predicted results of conversion versus time, composition versus conversion, and molecular weight development are compared against experimental data at different feed compositions. Diffusion-controlled effects and backbiting for BA were incorporated into the model as they proved to be significant in these polymerizations. The set of estimated global parameters allows one to assess the performance of these copolymerization systems over a wide range of monomer compositions.

Keywords: modeling; polymerization kinetics; n-butyl acrylate; methyl methacrylate; 2-ethylhexyl acrylate

1. Introduction

Copolymer synthesis is important in several areas due to the wide range of properties that can be achieved from the combination of different monomers. Potential applications for the materials that result from the virtually unlimited possible combinations have not been fully explored and studied [1]. Acrylate copolymers are of specific interest because of their widespread use in coatings, adhesives, resins, and many other products [1,2]. N-Butyl acrylate (BA), 2-ethyl hexyl acrylate (EHA), and methyl methacrylate (MMA) monomers are used in adhesive production and coating applications as binders in household paints [2,3] largely because their different glass transition temperatures allow for the control of adhesive and other mechanical properties [4,5].

The use of MMA and BA for polymerization processes has been studied abundantly. Their kinetic rate coefficients and the specific phenomena caused by their presence in polymerization recipes are well known and understood [6]. EHA, on the other hand, has not been studied to the same extent. Nonetheless, the propagation rate coefficient has been studied in bulk polymerizations at lower reaction temperatures (5–25 °C) [7]. Other studies in mini-emulsion [8] and micro-emulsion [9] polymerizations provide important comparative information on kinetic behavior. For example, the kinetic behavior of EHA was shown to be similar to that of BA in emulsion polymerizations at 75 °C [10]. The production of tertiary radicals resulting from transfer to polymer reactions, mostly due to backbiting reactions, was noted. The backbiting reactions led to a lower effective propagation rate coefficient. Extrapolation of the propagation rate coefficient from the bulk polymerization conditions (25 °C) of Beuermann et al. [7] to the emulsion polymerization conditions (75 °C) resulted in differing values from that estimated in the emulsion polymerization [10]. The backbiting reactions for EHA were shown to be higher than

that of BA in solution polymerizations at 70 °C [11]. Additional work in solution polymerization at low temperatures (−25–10 °C) showed a lower propagation rate coefficient than Beuermann et al. [7], leading to speculation that a possible solvent effect was present [12]. The most recent pulsed laser polymerization study in bulk by Junkers et al. [13] provides propagation rate coefficients in the temperature range 20 to 80 °C. Thus, aside from the propagation rate coefficient, detailed kinetic studies of free radical polymerization of EHA in bulk or modeling studies of such polymerizations are rare. The present contribution uses some recent data published by some of the co-authors to begin a more comprehensive look at modeling EHA-based copolymers [14]. More recent studies involving EHA in living polymerizations underlie the need for this kinetic modeling [15–18].

Diffusion-controlled (DC) effects, particularly the auto-acceleration effect which manifests at 30–50% monomer conversions, have proven to be of great importance for reliable modeling results in free-radical polymerization (FRP) [19]. Monomers that polymerize by FRP have been classified into two types, depending on the effect that DC-termination has on the polymerization rate [20]. Class "A" monomers, of which BA is a typical example, show a notorious increase in polymerization rate during the full conversion range. On the other hand, Class "B" polymers, of which MMA is a representative case, present a "plateau region" at low conversions, followed by the previously mentioned acceleration up to high conversions [21]. EHA was not included in that classification since it became important in more recent years, and it is usually polymerized in emulsion and solution processes. Therefore, DC effects in bulk polymerization of EHA have not been reported nor fully explored. In this contribution, DC effects have been considered in the copolymerization of BA, MMA and EHA.

Backbiting and the formation of tertiary radicals have been reported and measured in the polymerization of several acrylates [22,23], mainly BA, methyl acrylate (MA), EHA and dodecyl acrylate (DA). Backbiting for BA was included in our modeling approach because it has been reported to be important [24,25]. Although MMA is a widely studied monomer, there are no reports that we are aware of where backbiting is important for this monomer. In the case of EHA, there is evidence that backbiting may become important at temperatures in the range of 100 to 140 °C [23]. Since the experiments used in our study were conducted at 60 °C, it is well justified to neglect backbiting for EHA.

2. Experimental Section

The polymerization conditions and experimental data used herein are from a previous experimental study of the addressed systems [14]. Even though monomers were purified to remove inhibitors by passing them through an inhibitor removal column, significant inhibition periods were observed in all polymerizations. This result may be attributed to residual oxygen which was already present in the glass ampoules where the polymerizations were carried out. Since our model did not include this phenomenon, the experimental data were slightly modified to remove the effect. The correction procedure consisted of fitting a predefined function to the conversion-time profiles, extrapolating to zero conversion and adjusting data to the new zero condition. An example of this procedure is shown in Figure 1: Once the zero-conversion time was calculated with the empirical function (a logarithmic function in the example of Figure 1), the times corresponding to the experimental data were corrected by subtracting the calculated induction times to the recorded experimental ones. Each experimental data has its own induction time since it is virtually impossible to determine the exact amount of residual oxygen for every ampoule. The fitting functions were logarithmic, polynomial or linear.

$$\text{Adjusted time} = \text{Original time} - \text{Estimated induction time} \quad (1)$$

The polymerizations were carried out using azobisisobutyronitrile (AIBN), at a concentration of 0.08 wt.% in glass ampoules submerged in a temperature-controlled oil bath set to 60 °C, so that isothermicity can be assumed. Near-isothermal conditions have been reported for ampoule reactors of high surface to volume ratios at even higher AIBN concentrations [26]. Experimental monomer feed compositions for the three systems studied in this contribution (BA/EHA, MMA/EHA, BA/EHA/MMA) are detailed in Tables 1–3. The induction times fitting functions are summarized in Table 4.

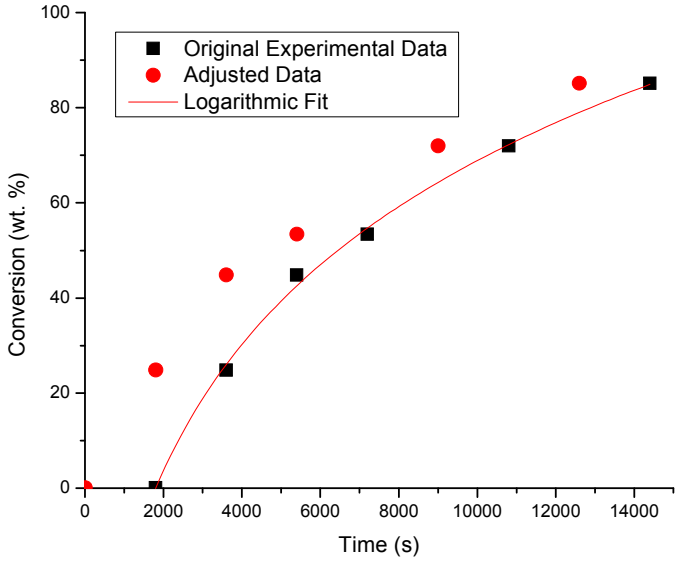

Figure 1. Comparison between original experimental data and adjusted data for BA-EHA copolymer with an initial 50/50 molar proportion.

Table 1. Experimental conditions for the bulk copolymerization of BA and EHA at 60 °C.

Monomer Feed (BA Molar Fraction)	Monomer Feed (EHA Molar Fraction)	BA (mol L^{-1})	EHA (mol L^{-1})	AIBN (mol L^{-1})
$f_{BA} = 0.3$	$f_{EHA} = 0.7$	1.596	3.699	0.00414
$f_{BA} = 0.5$	$f_{EHA} = 0.5$	2.844	2.836	0.00414
$f_{BA} = 0.7$	$f_{EHA} = 0.3$	4.284	1.837	0.00414

Table 2. Experimental conditions for the bulk copolymerization of MMA/EHA at 60 °C.

Monomer Feed (MMA Molar Fraction)	Monomer Feed (EHA Molar Fraction)	MMA (mol L^{-1})	EHA (mol L^{-1})	AIBN (mol L^{-1})
$f_{MMA} = 0.3$	$f_{EHA} = 0.7$	1.6847	3.9407	0.00414
$f_{MMA} = 0.5$	$f_{EHA} = 0.5$	3.1794	3.1762	0.00438
$f_{MMA} = 0.7$	$f_{EHA} = 0.3$	5.1093	2.1897	0.00438

Table 3. Experimental conditions for the bulk terpolymerization of BA, EHA and MMA at 60 °C.

Monomer Feed (BA Molar Fraction)	Monomer Feed (EHA Molar Fraction)	Monomer Feed (MMA Molar Fraction)	BA (mol L^{-1})	EHA (mol L^{-1})	MMA (mol L^{-1})	AIBN (mol L^{-1})
$f_{BA} = 0.8$	$f_{EHA} = 0.1$	$f_{MMA} = 0.1$	5.456	0.683	0.677	0.00414
$f_{BA} = 0.1$	$f_{EHA} = 0.8$	$f_{MMA} = 0.1$	0.512	4.207	0.509	0.00419
$f_{BA} = 0.1$	$f_{EHA} = 0.1$	$f_{MMA} = 0.8$	0.835	0.834	6.689	0.00450

Table 4. Estimated induction times and extrapolation functions for each polymerization.

System	r^2 Value	Fitting Equation (x: Conversion; t: Time)	Induction Time (s)
BA/50EHA	0.997	$x = 38.457\ln(t) - 288.17$	1796
30BA/70EHA	0.993	$x = 38.464\ln(t) - 278.76$	1404
70BA/30EHA	0.998	$x = 40.656\ln(t) - 303.78$	1758
50MMA/50EHA	0.996	$x = 7E{-}08t^2 + 0.002t - 3.0858$	1468
30MMA/70EHA	0.996	$x = 4E{-}08t^2 + 0.0034t - 4.8554$	1405
70MMA/30EHA	0.996	$x = 4E{-}08t^2 + 0.0025t - 4.1244$	1608
10BA/10MMA/80EHA	0.969	$x = 39.607\ln(t) - 293.78$	1665
10BA/80MMA/10EHA	0.987	$x = 0.0038t - 10.949$	2881
80BA/10MMA/10EHA	0.899	$x = 33.614\ln(t) - 251.67$	1785

3. Model Development

Tables 5–7 show the reaction steps used in PREDICI® (version 11.Hilbert.4, Computing in Technology, CiT, Rastede, Lower Saxony, Germany), a software commonly used in polymer science and engineering [27–29]. The copolymerization schemes for the three studied systems (BA/EHA, EHA/MMA, BA/EHA/MMA) are based on conventional bulk free-radical copolymerization kinetics, but takeinto consideration the nature of each system, such as the occurrence of certain side reactions (e.g., backbiting for BA [25], the presence of additional cross reactions for the terpolymer, and building on previous knowledge on MMA and BA homo- and copolymerizations [19,20,25].

Table 5. Polymerization scheme and kinetic rate coefficients used in PREDICI® for simulation of the bulk copolymerization of BA and EHA at 60 °C (M1 = BA, M2 = EHA).

Description	Step in PREDICI®	Parameter	Value (L mol^{-1} s^{-1} Unless Otherwise Stated)	Reference
Initiation				
Initiator decomposition	I→2fI•	*k*i, f	7.4609E−6, 0.58 (s^{-1})	[30]
First Propagation for BA	I• + M1→P1(1)	*k*p1	1333.8	[31]
First Propagation for EHA	I• + M2→P2(1)	*k*p2	33,395	[7]
Propagation				
Self-propagation for BA	P1(s)• + M1→P1(s+1)•	*k*p1	1333.8	[31]
Self-propagation forEHA	P2(s)• + M2→P2(s+1)•	*k*p2	33,395	[7]
Cross-Propagation	P1(s)• + M2→P2(s+1)•	*k*p12	1333.8/r12	[14,31]
Cross-Propagation	P2(s)• + M1→P1(s+1)•	*k*p21	33,395/r21	[7,14]
Chain Transfer				
Chain Transfer to BA	P1(s)• + M1→P(s) + P1(1)•	*k*f1	0.1492	[31]
Chain Transfer to BA	P2(s)• + M1→P(s) + P1(1)•	*k*f21	3.5/r21	This work/[14]
Chain Transfer to EHA	P1(s)• + M2→P(s) + P2(1)•	*k*f12	0.1492/r12	[14,31]
Chain Transfer to EHA	P2(s)• + M2→P(s) + P2(1)•	*k*f2	3.5	This work
Intramolecular chain transfer to BA				
Backbitingfor BA	P1(s)•→Q1(s)•	*k*bb	553	[32]
Short-chainbranching BA	Q1(s)• + M1→P1(s+1)•	*k*p1tert	49.401	[33]
Short-chainbranching EHA	Q1(s)• + M2→P2(s+1)•	*k*p12tert	49.401/r12	[14,33]
Degradativechain transfer	Q1(s)• + M1→P(s) + P1(1)•	*k*f1tert	6	This work
Degradativechain transfer	Q1(s)• + M2→P(s) + P2(1)•	*k*f12tert	6/r12	This work/[14]
Termination				
Bycombination	P1(s)• + P1(r)•→P(s+r)	*k*tc11	1.2259E6	[31]
-	P1(s)• + P2(r)•→P(s+r)	*k*tc21	√ktc11·ktc22	[31]/This work
-	P2(s)• + P2(r)•→P(s+r)	*k*tc22	2.5E8	This work
Bydisproportionation	P1(s)• + P1(r)•→P(s) + P(r)	*k*td11	8.5815E5	[31]
-	P1(s)• + P2(r)•→P(s) + P(r)	*k*td21	√ktd11·ktd22	[31]/This work
-	P2(s)• + P2(r)•→P(s) + P(r)	*k*td22	2.5E8	This work
Termination of BA tertiary radicals				
Bycombination	Q1(s)• + P1(r)•→P(s+r)	*k*tc11	1.2259E6	[31]
-	Q1(s)• + P2(r)•→P(s+r)	*k*tc21	√ktc11·ktc22	[31]/This work
-	Q1(s)• + Q1(r)•→P(s+r)	*k*tc11	1.2259E6	[31]
Bydisproportionation	Q1(s)• + P1(r)•→P(s) + P(r)	*k*td11	8.5815E5	[31]
-	Q1(s)• + P2(r)•→P(s) + P(r)	*k*td21	√ktd11·ktd22	[31]/This work
-	Q1(s)• + Q1(r)•→P(s) + P(r)	*k*td11	8.5815E5	[31]

Table 6. Polymerization scheme and kinetic rate coefficients used in PREDICI® for simulation of the bulk copolymerization of MMA and EHA at 60 °C (M1 = MMA, M2 = EHA).

Description	Step in PREDICI®	Parameters	Value (L mol^{-1} s^{-1}, Unless Otherwise Stated)	Reference
Initiation				
Initiator decomposition	I→2fI•	*k*i, f	7.4609E−6, 5.8E−1 (s^{-1})	[30]
First Propagation for MMA	I• + M1→P1(1)	*k*p1	683.24	[31]
First Propagation for EHA	I• + M2→P2(1)	*k*p2	33,395	[7]
Propagation				
Self-propagation for MMA	P1(s)• + M1→P1(s+1)•	*k*p1	683.24	[31]
Self-propagation for EHA	P2(s)• + M2→P2(s+1)•	*k*p2	33,395	[7]
Cross-Propagation	P1(s)• + M2→P2(s+1)•	*k*p12	683.24/r12	[14,31]
Cross-Propagation	P2(s)• + M1→P1(s+1)•	*k*p21	33,395/r21	[7,14]
Chain Transfer				
Chain Transfer to MMA	P1(s)• + M1→P(s) + P1(1)•	*k*f1	1.9321E−2	[31]
Chain Transfer to MMA	P2(s)• + M1→P(s) + P1(1)•	*k*f21	3.5/r21	This work/[14]
Chain Transfer to EHA	P1(s)• + M2→P(s) + P2(1)•	*k*f12	1.9321E−2/r12	[14,31]
Chain Transfer to EHA	P2(s)• + M2→P(s) + P2(1)•	*k*f2	3.5	This work
Termination				
By combination	P1(s)• + P1(r)•→P(s+r)	*k*tc11	1.859E7	[31]
-	P1(s)• + P2(r)•→P(s+r)	*k*tc21	√ktc11·ktc22	[31]/This work
-	P2(s)• + P2(r)•→P(s+r)	*k*tc22	2.5E8	This work
By disproportionation	P1(s)• + P1(r)•→P(s) + P(r)	*k*td11	1.5382E7	This work
-	P1(s)• + P2(r)•→P(s) + P(r)	*k*td21	√ktd11·ktd22	[31]/This work
-	P2(s)• + P2(r)•→P(s) + P(r)	*k*td22	2.5E8	This work

Table 7. Polymerization scheme and kinetic rate coefficients used in PREDICI® for simulation of the bulk copolymerization of BA, EHA and MMA at 60 °C (M1 = BA, M2 = EHA, M3 = MMA).

Description	Step in PREDICI®	Parameters	Value (L mol^{-1} s^{-1}, Unless Otherwise Stated)	Reference
Initiation				
Initiator decomposition	I→2fI•	*k*i, f	7.4609E−6, 0.58 (s^{-1})	[30]
First Propagation for BA	I• + M1→P1(1)	*k*p1	1333.8	[31]
First Propagation for EHA	I• + M2→P2(1)	*k*p2	33,395	[7]
First Propagation for MMA	I• + M3→P3(1)	*k*p3	683.24	[31]
Propagation				
Self-propagation for BA	P1(s)• + M1→P1(s+1)•	*k*p1	1333.8	[31]
Self-propagation for EHA	P2(s)• + M2→P2(s+1)•	*k*p2	33,395	[7]
Self-propagation forMMA	P3(s)• + M3→P3(s+1)•	*k*p3	683.24	[31]
Cross-Propagation	P1(s)• + M2→P2(s+1)•	*k*p12	1333.8/r12	[14,31]
Cross-Propagation	P1(s)• + M3→P3(s+1)•	*k*p13	1333.8/r13	[31,34]
Cross-Propagation	P2(s)• + M1→P1(s+1)•	*k*p21	33,395/r21	[7,14]
Cross-Propagation	P2(s)• + M3→P3(s+1)•	*k*p23	33,395/r23	[7,14]
Cross-Propagation	P3(s)• + M1→P1(s+1)•	*k*p31	683.24/r31	[31,34]
Cross-Propagation	P3(s)• + M2→P2(s+1)•	*k*p32	683.24/r32	[31,34]
Chain Transfer				
Chain Transfer to BA	P1(s)• + M1→P(s) + P1(1)•	*k*f1	0.1492	[31]
Chain Transfer to BA	P2(s)• + M1→P(s) + P1(1)•	*k*f21	3.5/r21	This work/[14]
Chain Transfer to BA	P3(s)• + M1→P(s) + P1(1)•	*k*f31	1.9321E−2/r31	[31,34]
Chain Transfer to EHA	P1(s)• + M2→P(s) + P2(1)•	*k*f12	0.1492/r12	[14,31]
Chain Transfer to EHA	P2(s)• + M2→P(s) + P2(1)•	*k*f2	4.5	This work
Chain Transfer to EHA	P3(s)• + M2→P(s) + P2(1)•	*k*f32	1.9321E−2/r32	[14,31]
Chain Transfer to MMA	P1(s)• + M3→P(s) + P3(1)•	*k*f13	0.1492/r13	[31,34]
Chain Transfer to MMA	P2(s)• + M3→P(s) + P3(1)•	*k*f23	3.5/r23	This work/[31]
Chain Transfer to MMA	P3(s)• + M3→P(s) + P3(1)•	*k*f3	1.9321E−2	[31]
Intramolecular chain transfer of BA				
Backbiting for BA	P1(s)•→Q1(s)•	*k*bb	553	[32]
Short-chain branching BA	Q1(s)• + M1→P1(s+1)•	*k*p1tert	49.401	[33]
Short-chain branching EHA	Q1(s)• + M2→P2(s+1)•	*k*p12tert	49.401/r12	[14,33]
Short-chain branching EHA	Q1(s)• + M3→P3(s+1)•	*k*p13tert	49.401/r13	[33,34]
Degradative chain transfer	Q1(s)• + M1→P(s) + P1(1)•	*k*f1tert	6	This work
Degradative chain transfer	Q1(s)• + M2→P(s) + P2(1)•	*k*f12tert	6/r12	This work/[14]
Degradative chain transfer	Q1(s)• + M3→P(s) + P3(1)•	*k*f13tert	6/r13	This work/[34]

Table 7. *Cont.*

Description	Step in PREDICI®	Parameters	Value (L mol^{-1} s^{-1}, Unless Otherwise Stated)	Reference
	Termination			
By combination	P1(s)• + P1(r)•→P(s+r)	*k*tc11	1.2259E6	[31]
-	P1(s)• + P2(r)•→P(s+r)	*k*tc21	√ktc11·ktc22	[31]/This work
-	P1(s)• + P3(r)•→P(s+r)	*k*tc31	√ktc11·ktc33	[31]
-	P2(s)• + P2(r)•→P(s+r)	*k*tc22	2.5E8	This work
-	P2(s)• + P3(r)•→P(s+r)	*k*tc32	√ktc22·ktc33	This work/[31]
-	P3(s)• + P3(r)•→P(s+r)	*k*tc33	1.859E7	[31]
By disproportionation	P1(s)• + P1(r)•→P(s) + P(r)	*k*td11	8.5815E5	[31]
-	P1(s)• + P2(r)•→P(s) + P(r)	*k*td21	√ktd11·ktd22	[31]/This work
-	P1(s)• + P3(r)•→P(s) + P(r)	*k*td31	√ktd11·ktd33	[31]
-	P2(s)• + P2(r)•→P(s) + P(r)	*k*td22	2.5E8	This work
-	P2(s)• + P3(r)•→P(s) + P(r)	*k*td32	√ktd22·ktd33	This work/[31]
-	P3(s)• + P3(r)•→P(s) + P(r)	*k*td33	1.5382E7	[31]
	Termination of BA tertiary radicals			
By combination	Q1(s)• + P1(r)•→P(s+r)	*k*tc11	1.2259E6	[31]
-	Q1(s)• + P2(r)•→P(s+r)	*k*tc21	√ktc11·ktc22	This work
-	Q1(s)• + P3(r)•→P(s+r)	*k*tc31	√ktc11·ktc33	[31]
-	Q2(s)• + Q2(r)•→P(s+r)	*k*tc22	2.5E8	This work
-	Q2(s)• + Q3(r)•→P(s+r)	*k*tc32	√ktc22·ktc33	This work/[31]
-	Q3(s)• + Q3(r)•→P(s+r)	*k*tc33	1.859E7	[31]
By disproportionation	Q1(s)• + P1(r)•→P(s) + P(r)	*k*td11	8.5815E5	[31]
-	Q1(s)• + P2(r)•→P(s) + P(r)	*k*td21	√ktd11·ktd22	[31]/This work
-	Q1(s)• + P3(r)•→P(s) + P(r)	*k*td31	√ktd11·ktd33	[31]
-	Q2(s)• + P2(r)•→P(s) + P(r)	*k*td22	2.5E8	This work
-	Q2(s)• + P3(r)•→P(s) + P(r)	*k*td32	√ktd22·ktd33	This work/[31]
-	Q3(s)• + Q3(r)•→P(s) + P(r)	*k*td33	1.5382E7	[31]

3.1. Initiation

The initiation reaction involves two steps, as shown in Equations (2) and (3).

$$I \rightarrow 2fI^{\bullet} \quad (2)$$

$$I^{\bullet} + M_i \rightarrow P_i(1) \quad (3)$$

As with many other initiators, AIBN decomposes into two initiator primary free radicals ($I^{\bullet}$). The Arrhenius expression for the initiator decomposition kinetic rate coefficient is given by Equation (4) [6,31].

$$k_i\ (s^{-1}) = 1.07E14\exp(-1.515 \times 10^4/T) \quad (4)$$

The initiator primary free radicals react with either of the monomers producing polymer radicals of each type and size 1. Since not all initiator molecules produce primary free radicals due to side reactions, an efficiency factor (f) for initiation is required. One explanation for the use of f is the so-called "cage effect", which allows us to avoid considering side reactions such as termination between primary free radicals [35]. A value of $f = 0.58$ was used [30].

3.2. Propagation

Since the polymerization scheme is based on the terminal model [1], four propagation and four-chain transfer to monomer reactions are involved. The self-propagation kinetic rate coefficients for MMA and BA are shown in Equations (5) and (6) [6,31]. The cross-propagation kinetic rate coefficients are expressed in terms of reactivity ratios, as detailed in Section 3.4.

$$kp_{\underline{\mathrm{MMA}}}(\mathrm{L\ mol^{-1}\ s^{-1}}) = 4.917E5\exp(-4.353 \times 10^3/T) \quad (5)$$

$$kp_{\mathrm{BA}}(\mathrm{L\ mol^{-1}\ s^{-1}}) = 2.767E9\exp(-9.630 \times 10^3/T) \quad (6)$$

For the EHA, the self-propagation kinetic rate coefficient and pulsed laser polymerization (PLP) experimental data [7] were analyzed and adjusted to an Arrhenius relationship, leading to Equation (7).

The value for kp_{EHA} used in our simulations (Table 5) is consistent (order of magnitude agreement) with values reported in other studies for such parameters at the same temperature [13].

$$kp_{\mathrm{EHA}}(\mathrm{L\ mol^{-1}\ s^{-1}}) = 9.00\mathrm{E6exp}(-3.694 \times 10^3/\mathrm{T}) \tag{7}$$

3.3. Chain Transfer

Kinetic rate coefficients for chain transfer to MMA and BA are given by Equations (8) and (9) [6,31].

$$kf_{\mathrm{MMA}}(\mathrm{L\ mol^{-1}\ s^{-1}}) = 1.55\mathrm{E4exp}(-7.475 \times 10^3/\mathrm{T}) \tag{8}$$

$$kf_{\mathrm{BA}}(\mathrm{L\ mol^{-1}\ s^{-1}}) = 1.55\mathrm{E3exp}(-7.475 \times 10^3/\mathrm{T}) \tag{9}$$

Unfortunately, there was no reliable information in the literature for chain transfer to EHA kinetic rate coefficients in bulk polymerization. A value of kf_{BA} = 3.5 L mol^{-1} s^{-1} at 60 °C was estimated in this contribution.

The cross-chain transfer kinetic rate coefficients were obtained using reactivity ratios as in the case of propagation.

3.4. Cross-Propagation and Cross-Chain Transfer

Reactivity ratios, defined by Equation (10), were used to calculate the cross-parameters.

$$r_{12} = \frac{k_{p1}}{k_{p12}} = \frac{k_{f1}}{k_{f12}};\ r_{21} = \frac{k_{p2}}{k_{p21}} = \frac{k_{f2}}{k_{f21}} \tag{10}$$

The reactivity ratios for BA/EHA, MMA/EHA and BA/EHA/MMA used in our calculations are summarized in Equations (11)–(15), and were taken from the composition results obtained from Gabriel and Dubé [14] (at 60 °C) using a computational package developed in MATLAB [36].

BA/EHA

$$r_{12} = \frac{k_{BA}}{k_{EHA}} = \frac{k_{p1}}{k_{p12}} = \frac{k_{f1}}{k_{f12}} = 0.994;\ r_{21} = \frac{k_{EHA}}{k_{BA}} = \frac{k_{p2}}{k_{p21}} = \frac{k_{f2}}{k_{f21}} = 1.621 \tag{11}$$

MMA/EHA

$$r_{12} = \frac{k_{MMA}}{k_{EHA}} = \frac{k_{p1}}{k_{p12}} = \frac{k_{f1}}{k_{f12}} = 1.496;\ r_{21}\frac{k_{EHA}}{k_{MMA}} = \frac{k_{p2}}{k_{p21}} = \frac{k_{f2}}{k_{f21}} = 0.315 \tag{12}$$

BA/EHA/MMA

$$r_{12} = \frac{k_{BA}}{k_{EHA}} = \frac{k_{p1}}{k_{p12}} = \frac{k_{f1}}{k_{f12}} = 0.994;\ r_{21} = \frac{k_{EHA}}{k_{BA}} = \frac{k_{p2}}{k_{p21}} = \frac{k_{f2}}{k_{f21}} = 1.621 \tag{13}$$

$$r_{13} = \frac{k_{BA}}{k_{MMA}} = \frac{k_{p1}}{k_{p13}} = \frac{k_{f1}}{k_{f13}} = 2.022;\ r_{31} = \frac{k_{MMA}}{k_{BA}} = \frac{k_{p2}}{k_{p31}} = \frac{k_{f2}}{k_{f31}} = 0.343 \tag{14}$$

$$r_{32} = \frac{k_{MMA}}{k_{EHA}} = \frac{k_{p1}}{k_{p32}} = \frac{k_{f1}}{k_{f32}} = 1.496;\ r_{23} = \frac{k_{EHA}}{k_{MMA}} = \frac{k_{p2}}{k_{p31}} = \frac{k_{f2}}{k_{f31}} = 0.315 \tag{15}$$

The reliability of reactivity ratios is fundamental for the accurate prediction of copolymer composition. As stated in the Mayo-Lewis equation, reactivity ratios are a measure of a monomer's preference and tendency to bond [35]. In the case of cross chain transfer to monomer reactions, since the reacting species are the same as in cross propagation, it was assumed that the cross chain transfer reactions can be calculated using the same reactivity ratios. This assumption does not have a strong theoretical background, but it allowed us to reduce the number of estimated parameters.

3.5. Backbiting of BA and Reactions with Mid-Chain Tertiary Radicals

Intramolecular chain transfer to polymer in BA polymerization is known to be important [37,38]. Mid-chain tertiary polymer radicals are formed from backbiting. They are quite stable and can propagate, transfer and terminate as any other polymer radicals. Backbiting and tertiary radical propagation, as well as their corresponding kinetic rate coefficients, are given by Equations (16)–(19) [25].

Tertiary radical formation:

$$\mathrm{P1(s)}\bullet \overset{kbb}{\rightarrow} \mathrm{Q1(s)}\bullet \tag{16}$$

$$k_{bb}\ (\mathrm{L\ mol^{-1}s^{-1}}) = 3.87 \times 10^{6}\exp(-2.299 \times 10^{3}/\mathrm{T}) \tag{17}$$

Tertiary radical propagation:

$$\mathrm{Q1(s)}\bullet + \mathrm{M1} \overset{kp1tert}{\rightarrow} \mathrm{P1(s+1)}\bullet \tag{18}$$

$$k_{p1tert}(\mathrm{L\ mol^{-1}\ s^{-1}}) = 59.9\exp(-64.2/\mathrm{T}) \tag{19}$$

Cross-propagation kinetic rate coefficients were also obtained from BA/EHA and BA/EHA/MMA reactivity ratios, which are given by Equations (20) and (21), respectively.

$$r_{12} = \frac{k_{BA}}{k_{EHA}} = \frac{k_{p1}}{k_{p12}} = \frac{k_{f1}}{k_{f12}} = 0.994; kp_{12tert} = \frac{k_{p1tert}}{r_{12}}; kf_{12tert} = \frac{k_{f1tert}}{r_{12}} \tag{20}$$

$$r_{13} = \frac{k_{BA}}{k_{MMA}} = \frac{k_{p1}}{k_{p13}} = \frac{k_{f1}}{k_{f13}} = 2.022; kp_{13tert} = \frac{k_{p1tert}}{r_{13}}; kf_{13tert} = \frac{k_{f1tert}}{r_{13}} \tag{21}$$

There were no estimates of k_{f1tert} reported in the literature. It was therefore estimated in this study ($k_{f1tert} = 6$).

3.6. Termination

Termination by combination and disproportionation kinetic rate coefficients for BA and MMA copolymerizations were also taken from WATPOLY, as shown in Equations (22) and (23) [6,31].

$$k_{tc\mathrm{MMA}} + k_{td\mathrm{MMA}}(\mathrm{L\ mol^{-1}\ min^{-1}}) = 4.68 \times 10^{8}\exp(-8.73 \times 10^{2}/\mathrm{T}) \tag{22}$$

$$k_{tc\mathrm{BA}} + k_{td\mathrm{BA}}(\mathrm{L\ mol^{-1}\ min^{-1}}) = 5.88 \times 10^{9}\exp(-7.01 \times 10^{2}/\mathrm{T}) \tag{23}$$

The ratio between both termination kinetic rate coefficients for MMA and BA copolymerizations is given by Equation (24) [14].

$$\frac{k_{tcMMA}}{k_{tdMMA}} = 0.8275;\ \frac{k_{tcBA}}{k_{tdBA}} = 0.7000 \tag{24}$$

Termination by combination and disproportionation kinetic rate coefficients for EHA were estimated in this work, obtaining the values shown in Equations (25) and (26).

$$ktc_{EHA} + ktd_{EHA} = 5 \times 10^{8} \tag{25}$$

$$ktc_{EHA} = ktd_{EHA} = 2.5 \times 10^{8} \tag{26}$$

The missing "cross-termination" constants were calculated using the geometric average for every specific case, as shown in Equation (27).

$$kt_{ij} = \sqrt{kt_i kt_j} \tag{27}$$

In the case of bimolecular radical termination including mid chain radicals, Q1(s)•, it was assumed that $k_{t\mathrm{BA}}$ is independent of radical type [25,39]. More experimental or theoretical studies on termination of tertiary radicals to provide a sounder estimation of $k_{t\mathrm{BA}}$ would be useful. Until then, the assumption of independence of radical type is needed to simplify our parameter estimation approach. Therefore, the termination kinetic rate coefficients for such cases are the same as "cross-termination".

3.7. Diffusion-Controlled Effects

When implementing our model and trying to fit our experimental data, it was evident that diffusion-controlled (DC) effects were important. Since MMA was one of the monomers present in our reacting systems, this was not surprising [21,30]. All the reactions involving polymer molecules were assumed to be diffusion-controlled. DC effects were addressed using free-volume theory [25,40], as shown in Equation (28), where β is a free volume parameter andv_f is fractional free volume, defined by Equation (29). Subscript "0" stands for initial conditions. T and T_{gi} are the reaction temperature and glass transition temperature for component i (monomer or polymer of each of the possible species, BA, EHA or MMA); α_i is the expansion coefficient for species i, V_i is the volume of species i, and $V_t$is total volume.

$$k_i = k_i^o \exp\left[-\beta\left(\frac{1}{v_f} - \frac{1}{v_f^o}\right)\right] \tag{28}$$

$$v_f = \sum_{i=1}^{\#\ of\ components} \left[0.025 + \alpha_i\left(T - T_{gi}\right)\right]\frac{V_i}{V_t} \tag{29}$$

The free volume parameters used in our calculations for the three copolymerization systems are summarized in Tables 8 and 9. As observed in Table 9, different β values were required, even for similar polymer molecules, in order to explain the behavior observed experimentally over a wide range of (binary) copolymer and terpolymer compositions. This is not surprising if one considers that the material properties of the reacting mixture, such as viscosity [41], depend on molecular weight development but also on copolymer content in the reactive mass and quite likely, copolymer composition.

It is observed in Table 9 that β for kinetic rate coefficients with the same name differs from system to system. This is a consequence of the nomenclature used for each system. For instance, kp1 refers to BA in the case of copolymerization of BA and EHA, whereas the same parameter is related to MMA in the copolymerization of MMA and EHA. Also, DC effects in both propagation and termination reactions were required for the copolymerization of BA and EHA whereas only diffusion-controlled termination was needed in the case of copolymerization of MMA and EHA. High values of β result in an earlier and more pronounced decrease of the corresponding kinetic rate coefficient, while kinetic rate coefficients where no DC effects are considered remain constant throughout the polymerization.

In general, the presence of MMA causes higher polymerization rates. This behavior can be captured by the model by increasing β for termination or decreasing the corresponding β parameter for the propagation reaction. In other words, the β_t/β_p ratio for MMA must be greater (compared to the other monomers) for accurate predictions. The same trend applies for the "cross" kinetic rate coefficients when MMA is involved; β_t/β_p is also fundamental to tune the "onset" of the auto-acceleration effect. As discussed in the following section, it turned out that the only way to capture the behavior of the experimental data (particularly the conversion versus time profiles) was to include DC effects in most of the reactions and using different β values for similar polymer molecules.

Table 8. Free volume parameters used in our calculations.

Species	T_{gM}(K)	T_{gP}(K)	α_M	α_P
BA	185	218	0.001	0.00048
EHA	167	223	0.001	0.00048
MMA	167	387	0.001	0.00048

Table 9. β parameters used in our simulations; β = 0 implies that DC effects were neglected in such cases.

System	Rate Coefficients Where DC Effects Were Considered	β Value	Rate Coefficients Where DC Effects Were Neglected (β = 0)
BA-EHA	kp1	0.25	ki
	kp2	0.25	f
	kp12	0.25	*k*f1
	kp21	0.5	*k*f21
	kbb	5	*k*f12
	ktc11	4	*k*f2
	ktc21	0.5	*k*p1tert
	ktc22	2	*k*p12tert
	ktd11	4	*k*f1tert
	ktd21	0.5	*k*f12tert
	ktd22	2	—
MMA-EHA	kp2	0.5	ki
	kf1	1	f
	kf12	1	kp1, kp12
	kf2	1	kp2, kp21
	kf21	1	ktc22, ktd22
	ktc11	4	ktc21, ktd21
	ktd11	4	—
BA-EHA-MMA	kp1	1	ki
	kp12	1	f
	kp2	1.5	*k*f1
	kp21	1	*k*f21
	kp23	2	*k*f31
	kp13	2	*k*f12
	kp3	2	*k*f2
	kp31	2	*k*f32
	kp32	2	*k*f13
	kbb	2.5	*k*f23
	kf3	2	*k*bb
	kf13tert	2	*k*p1tert
	ktc11	6	*k*p12tert
	ktc21	2	*k*p13tert
	ktc22	2	*k*f1tert
	ktc31	10	*k*f12tert
	ktc32	10	—
	ktc33	10	—
	ktd11	6	—
	ktd21	2	—
	ktd22	2	—
	ktd31	10	—
	ktd32	10	—
	ktd33	10	—

3.8. Parameter Estimation Strategy

Most of the kinetic rate coefficients used in our study came from reports available in the literature. The kinetic rate coefficients estimated by us are summarized in Table 10. The other estimated parameters are the βs indicated in Table 9. As explained earlier, all the parameters estimated in this work are related to EHA. The estimation procedure consisted of a combination between a careful literature review, detailed parameter sensitivity analyses and the use of educated guesses (trial and error guided from the information gained from the literature review and the parameter sensitivity analyses). An example of the parameter estimation strategy is shown in Appendix A.

In the case of bimolecular radical termination between polymer radicals terminated in EHA monomer units, it was assumed that $ktc_{EHA} = ktd_{EHA}$. This is of course an approximation, but it is sufficient since, in many instances, in our model it is the total termination kinetic rate coefficient (kt = ktd + ktc) which is needed.

Table 10. Estimated kinetic rate coefficients in this work.

Parameter	Value	Description
ktc_{EHA}	2.5×10^8	EHA termination by combination
ktd_{EHA}	2.5×10^8	EHA termination by disproportionation
kf_{EHA}	45	Chain transfer to EHA
$kftert_{EHA}$	60	EHA intramolecular chain transfer to BA tertiary radicals
$kftert_{MMA}$	35	MMA intramolecular chain transfer to BA tertiary radicals

Regarding chain transfer to a monomer, our parameter sensitivity analyses showed that kf_{EHA}, $kftert_{EHA}$ and $kftert_{MMA}$ had a negligible effect on the polymerization rate, but that reaction is important for molecular weight development. Thus, initial guesses for these parameters were assigned order of magnitude estimates, based on values of that parameter for other monomers, and they were fine-tuned using molecular weight development experimental data. Our parameter estimation strategy included addressing the BA/EHA and MMA/EHA copolymer systems first, and then proceeding with the terpolymer case. Although we could get fairly good (order of magnitude) overall predictions of the polymerization rate, copolymer composition and molecular weight development for most of the cases studied by adjusting the intrinsic kinetic rate coefficients, the reproduction of unusual behavior (e.g., opposite trends in the conversion-time profiles when changing feed composition, overlap of profiles in certain instances, for system MMA/EHA) was possible only if strong DC effects (large β values) were used in some cases.

4. Results and Discussion

4.1. Conversion versus Time Profiles

As observed in Figures 2–4, good agreement between experimental data and calculated profiles of conversion versus time was obtained for all the conditions studied of the three copolymerization systems analyzed in this contribution. It is also observed from the experimental profiles for the three reacting systems that the polymerization rate is higher, and higher conversions are reached when EHA is present in a major proportion. This is consistent with the fact that kp for EHA turned out to be the highest for the three monomers considered in this study.

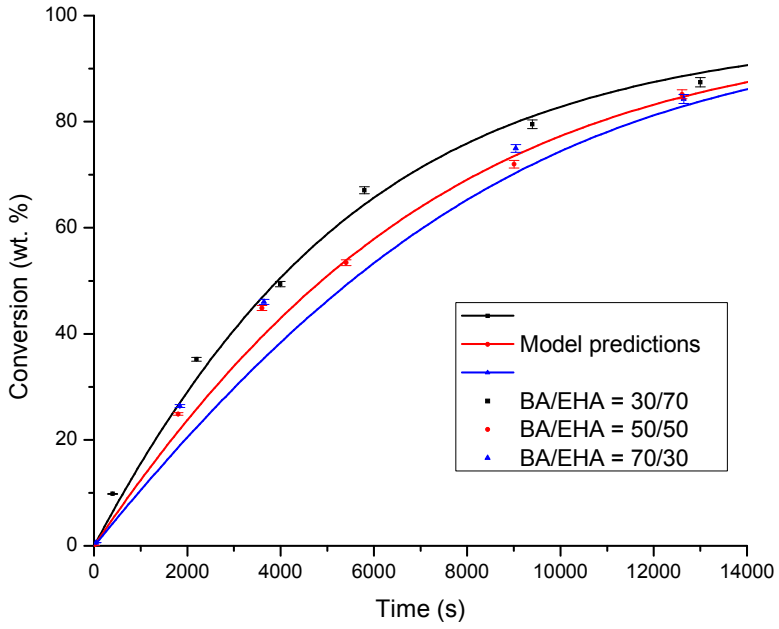

Figure 2. Comparison of experimental and calculated profiles of total monomer conversion versus time at 60 °C for copolymerization of BA and EHA at different initial concentrations of BA.

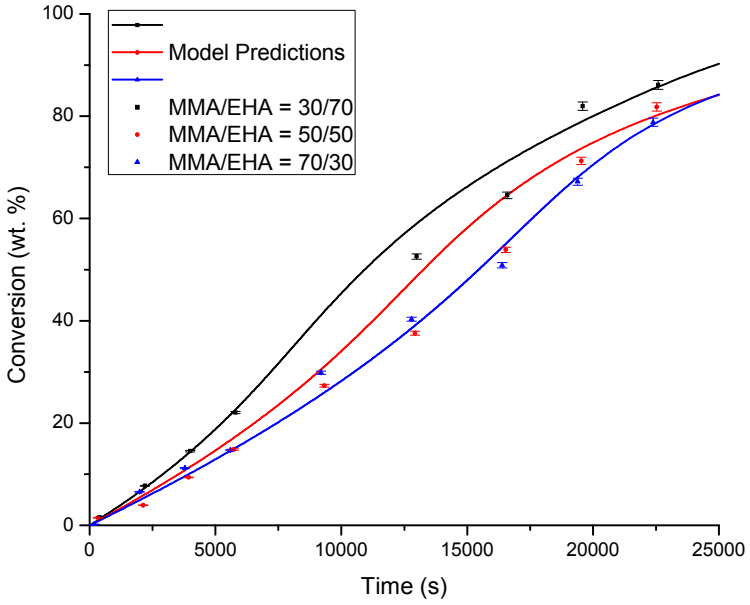

Figure 3. Comparison of experimental and calculated profiles of total monomer conversion versus time at 60 °C for copolymerization of MMA and EHA at different initial concentrations of MMA.

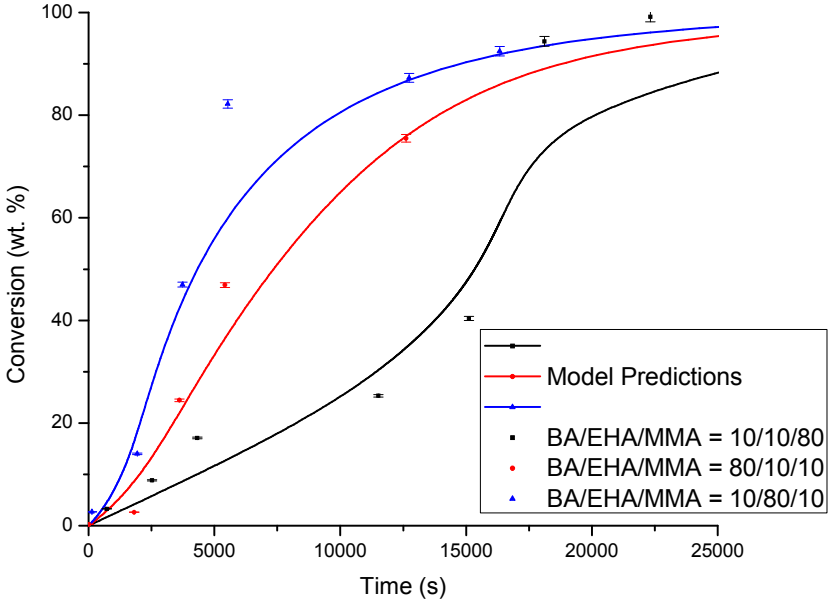

Figure 4. Comparison of experimental and calculated profiles of total monomer conversion versus time at 60 °C for copolymerization of BA, EHA and MMA at different initial concentrations.

If one compares the BA/EHA and MMA/EHA copolymerization systems, as shown in Figures 2 and 3, it is observed that BA polymerizes faster than MMA and EHA polymerizes faster than BA. As observed in the previous section, the kp values are consistent with these observations.

In the case of copolymerization of BA and EHA, it is observed in Figure 2 that higher polymerization rates are obtained when the amount of EHA is increased. However, that increase in polymerization rate is only marginal since the profiles are close to one another. This result can be explained by comparing kp and kt for both monomers. Although kp for EHA is almost one order of magnitude higher than kp for BA, kt for EHA is two orders of magnitude higher than kt for BA. Since the polymerization rate is proportional to kp and inversely proportional to $kt^{0.5}$, their effects almost cancel out. However, it is strange to observe from the experimental data that the final conversion for case 50BA/50EHA was higher than in case 70BA/30EHA, when the trend was exactly the opposite at very low conversions.

This effect could not be captured by the model without DC effects. Even when single β parameters for similar polymer molecules were used, the observed trend could not be replicated. The only way to capture this effect was to use different β and kt values for EHA (see summary of β parameters in Table 9). Additional experimental data (i.e., extending the experimental study to include other monomer compositions for each co- and terpolymer system) as well as EHA homopolymerization studies would be required to more accurately estimate the model parameters. Another possible explanation for the extra fine tuning of EHA parameters is the fact that we estimated induction times and corrected the experimental sampling times accordingly.

Similar behavior as the one described above is observed in Figure 3 for the copolymerization of MMA and EHA. Although more noticeable differences in the polymerization rate are observed in this case, these differences are still moderate. As observed for the BA/EHA system, in the case of copolymerization of MMA and EHA, the experimental data show higher conversion values in the very low conversion region and lower final conversions in the medium to high conversion regions for system 70MMA/30EHA, compared to system 50MMA/50EHA. The same explanation as in BA/EHA applies for MMA/EHA. Another important aspect observed in Figure 3 for the copolymerization of MMA and EHA is the presence of strong DCEs, particularly the auto-acceleration effect (typical "S"-shaped conversion versus time profiles, both experimental and calculated). This auto-acceleration effect (diffusion-controlled termination) is manifested in all the copolymerizations where MMA is present, even the case with the lowest content of MMA (30MMA/70EHA). As a matter of fact, this case with the lowest MMA content is the one wherethe strongest diffusion-controlled termination is observed (see Figure 3). This behavior can be explained by the large difference in propagation kinetic rate coefficients between the two monomers (kp for EHA is 2 orders in magnitude higher than kp for MMA), so that a decrease in termination will have a more noticeable effect in the species with the faster propagation. Accurate estimation of ktin our MMA-containing copolymerizations is quite important, given their lower propagation rates and the nature of the experimental results obtained, which show very similar conversions reached at quite different initial monomer concentrations.

As shown in Figure 4 for the terpolymerization of BA, EHA and MMA, more noticeable differences in the polymerization rate expressed as conversion versus time at different comonomer initial compositions are observed in this case, compared to the binary copolymerization systems analyzed earlier. These differences can again be explained in terms of different propagation rates among the three monomers (with EHA being the fastest monomer), but also by the monomer initial concentrations, where one monomer dominates the process. A close look at the β values reported in Table 9 shows again that DC effects and specifically diffusion-controlled termination are relevant for MMA, since higher β values are obtained for kinetic rate coefficients involving MMA and MMA cross interactions. As a matter of fact, the best overall fit to experimental data was obtained when system 10BA/10EHA/80MMA was used to estimate free volume parameters for MMA (estimation of β values for MMA related reactions).

4.2. Evolution of Kinetic Rate Coefficients Due to DC Effects

It was stated above that DC effects were needed to reproduce the observed experimental phenomena, particularly the effect of feed comonomer composition on the polymerization rate and molecular weight development. In order to understand such behavior, it is useful to visualize how the kinetic rate coefficients that are DC evolve over time. The evolution with conversion of kp and kt for system 30BA/70EHA, kp and kt for system 70EHA/30MMA, kp for system 10BA/10EHA/80MMA, kp for system 80BA/10EHA/10MMA, kp for system 10BA/80EHA/10MMA, kt for system 10BA/10EHA/80MMA, kt for system 80BA/10EHA/10MMA, and kt for system 10BA/80EHA/10MMA, are shown in Figures 5–12, respectively.

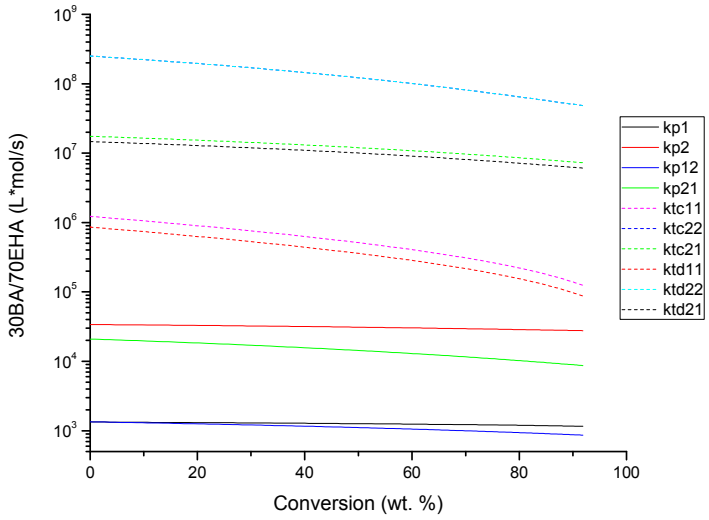

Figure 5. Evolution with conversion of propagation and termination kinetic rate coefficients for system 30BA/70EHA due to DCeffects.

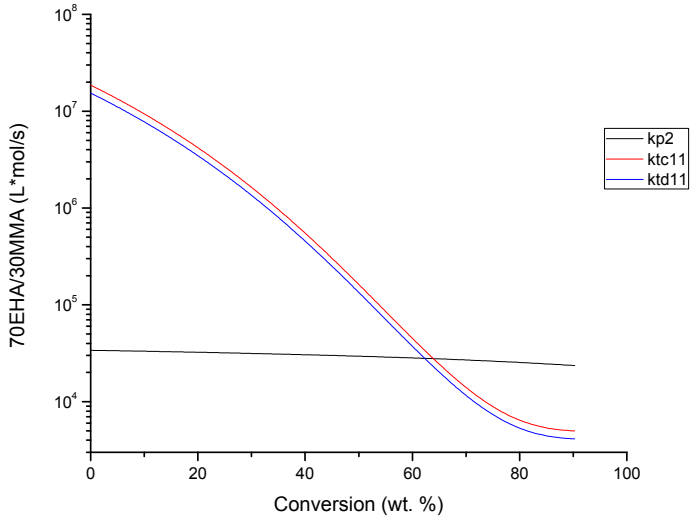

Figure 6. Evolution with conversion of propagation and termination kinetic rate coefficients for system 70EHA/30MMA due to DCeffects.

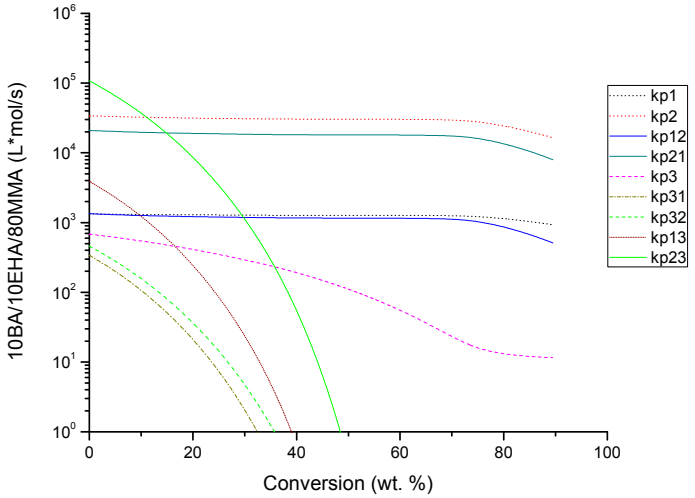

Figure 7. Evolution with conversion of propagation kinetic rate coefficient for system 10BA/10EHA/80MMA due to DCeffects.

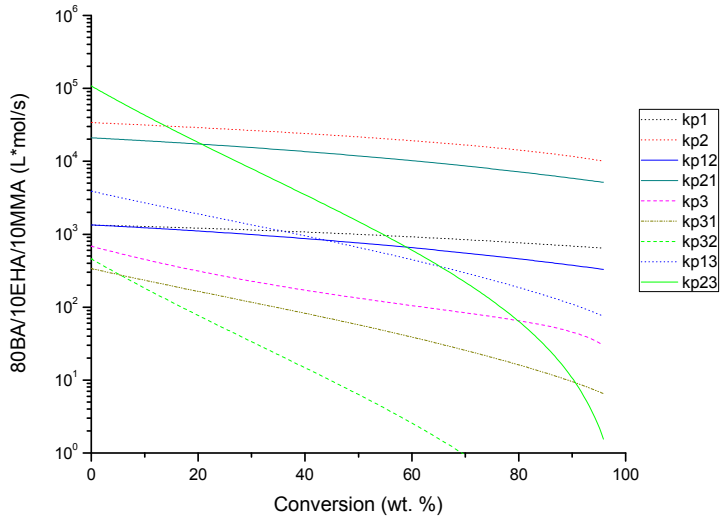

Figure 8. Evolution with conversion of propagation kinetic rate coefficient for system 80BA/10EHA/10MMA due to DCeffects.

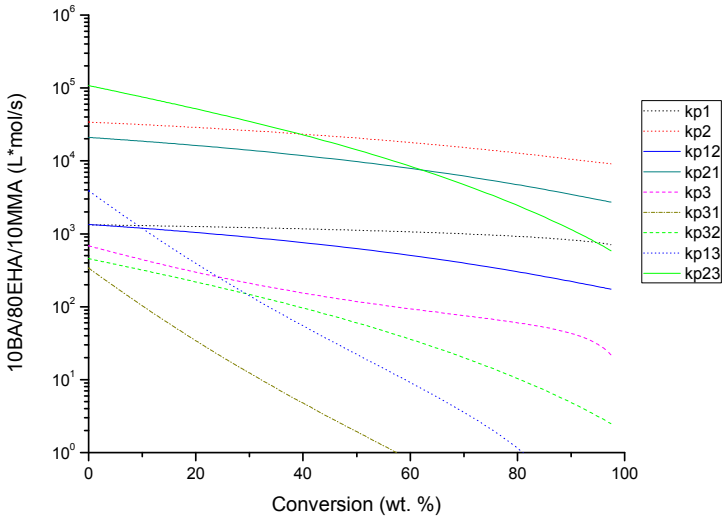

Figure 9. Evolution with conversion of propagation kinetic rate coefficient for system 10BA/80EHA/10MMA due to DCeffects.

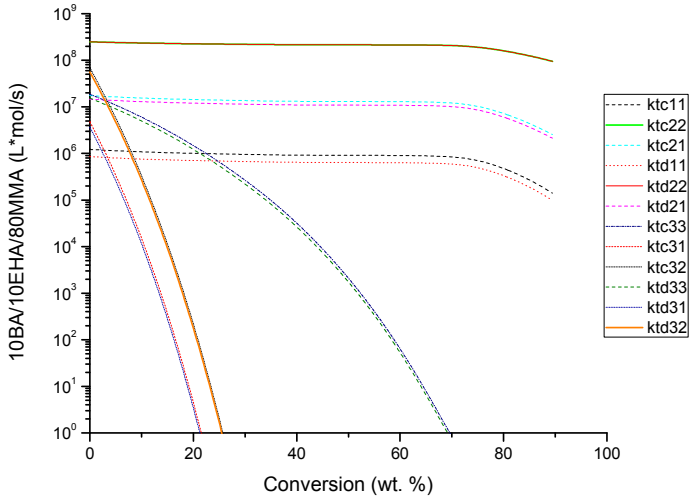

Figure 10. Evolution with conversion of termination kinetic rate coefficient for system 10BA/10EHA/80MMA due to DCeffects.

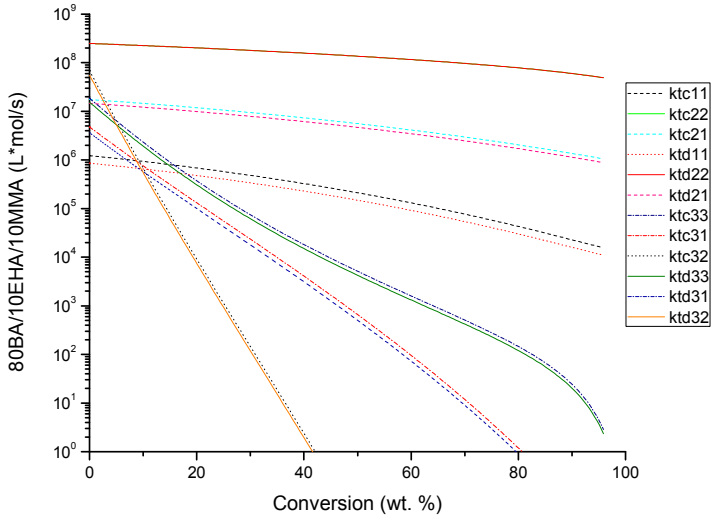

Figure 11. Evolution with conversion of termination kinetic rate coefficient for system80BA/10EHA/10MMA due to DCeffects.

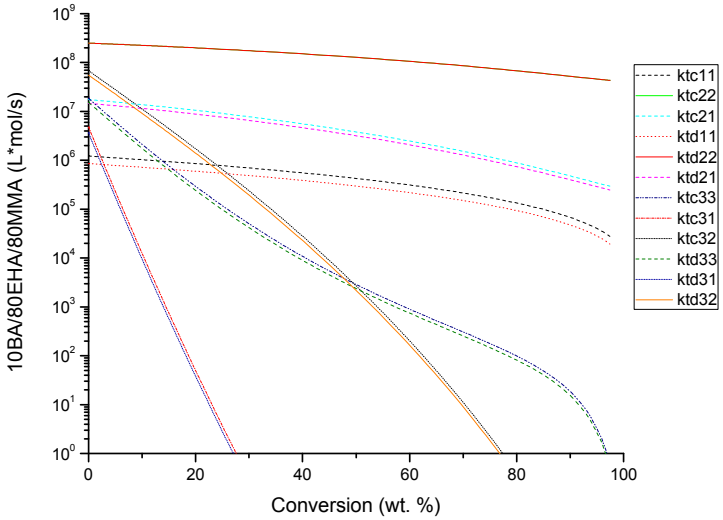

Figure 12. Evolution with conversion of termination kinetic rate coefficient for system10BA/80EHA/10MMA due to DCeffects.

It is observed in Figure 5 that kt and kp for system 30BA/70EHA decrease very slowly as conversion increases, remaining almost constant during the polymerization. This behavior is typical of systems with very weak DC effects and agree well with the conversion versus time profile shown in Figure 2 for the same copolymerization system. Figure 6, on the other hand, shows the behavior of system 70EHA/30MMA, which displays strong DCeffects. DCtermination is particularly strong for system 70EHA/30MMA, since kp decreases moderately, but kt decreases by several orders of magnitude. This behavior agrees well with the conversion versus time profile shown in Figure 3. Similar behavior was obtained for systems 50BA/50EHA, 70BA/30EHA, 50EHA/50MMA and 30EHA/70MMA, although results for those systems were not included here due to space considerations.

It is also observed in Figures 5 and 6, and in Table 9, that system BA/EHA required estimating more β parameters than system MMA/EHA. This is related to the nature of each system. System MMA/EHA is governed by the strong auto-acceleration effect (DC termination) of MMA whereas system BA/EHA required to estimate β parameters for several reactions involving polymer molecules in order to reproduce the experimental behavior of that system.

The terpolymer systems showed more complex behavior than the binary copolymerization ones. As observed in Figures 7–12 for the terpolymer systems, each case shows remarkably different behavior.

For instance, as observed in Figure 7, kp3, kp31, kp32, kp13 and kp23 for system 10BA/10EHA/80MMA decay much faster than in the other terpolymer systems shown in Figures 8 and 9. The common feature in those cases is that the involved kinetic rate coefficients are related to MMA and cross propagation reactions with MMA, a monomer with strong DC effects. Similar decaying behavior for the termination kinetic rate coefficients, particularly kt33, kt32 and kt31 (both combination and disproportionation), all of them related to MMA, once more, can be observed in Figures 10–12. This DC dependency of kp and k_t for the terpolymer systems agrees well with the conversion versus time profiles observed in Figure 4.

4.3. Copolymer Composition versus Conversion Profiles

As expected, accurate predictions of copolymer composition versus conversion strongly depend on the reactivity ratios used in the calculations. Given the excellent agreement between experimental data and calculated profiles of copolymer composition versus conversion at several initial compositions for the copolymerizations of BA and EHA, as well as MMA/EHA (see Figures 13 and 14), it is fair to say that the estimates of reactivity ratios for such systems [14] were very good.

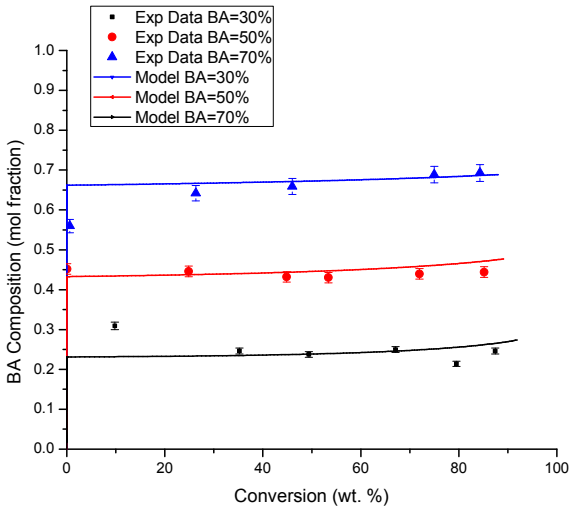

Figure 13. Comparison of experimental data and calculated profiles of BA composition versus conversion in the copolymerization of BA and EHA at different initial compositions of BA.

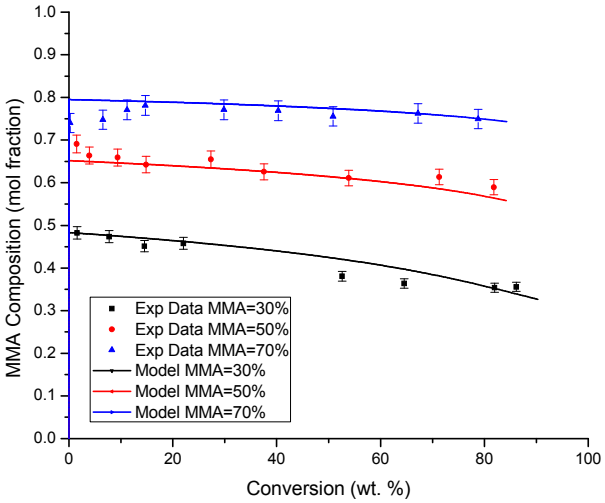

Figure 14. Comparison of experimental data and calculated profiles of MMA composition versus conversion in the copolymerization of MMA and EHA at different initial compositions of MMA.

However, as observed in Figures 15–17, the same does not hold entirely true for the terpolymerization cases. The agreement between experimental data and model predictions of copolymer

composition versus conversion for terpolymerizations 80BA/10EHA/10MMA (see Figure 17) and 10BA/80EHA/10MMA (see Figure 16) is very good, but it is poor for case 10BA/10EHA/80MMA, as observed in Figure 15. On a first thought, one may argue that better reactivity ratio estimates may be needed, particularly for MMA-BA interactions. It is observed in Figure 15 that the largest deviation between experimental data and model predictions occurs when initial MMA content is highest. Given the lower k_p value for MMA, compared to the corresponding values for BA and EHA, it may be argued that MMA incorporates slower into the copolymer and its composition could be slightly lower, as observed in the experimental profile (solid squares) of Figure 15. The adjustments carried out to eliminate induction times from experimental data may be an issue here. However, on a closer look, it is inferred from Table 9, that although the reactivity ratios at zero conversion coincide with the available ones, the fact that different free volume parameters (β values) for the cross-propagation terms were used, that causes the ratios to change (according to Equation (29); ratios of $k_{pi}{}^0$ remain unchanged, but since the βs are different, the actual ratios do not remain constant).

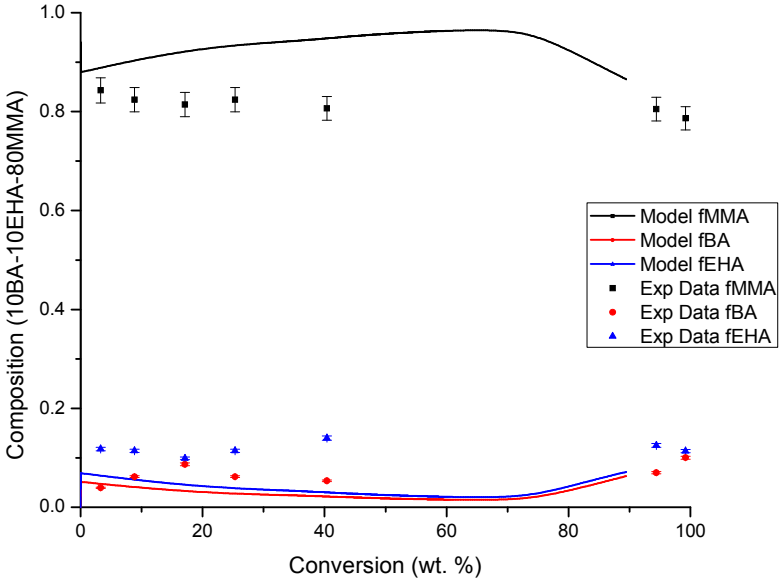

Figure 15. Comparison of experimental data and calculated profiles of copolymer composition for each monomer species versus conversion for a system with 10BA/10EHA/80MMA initial concentrations.

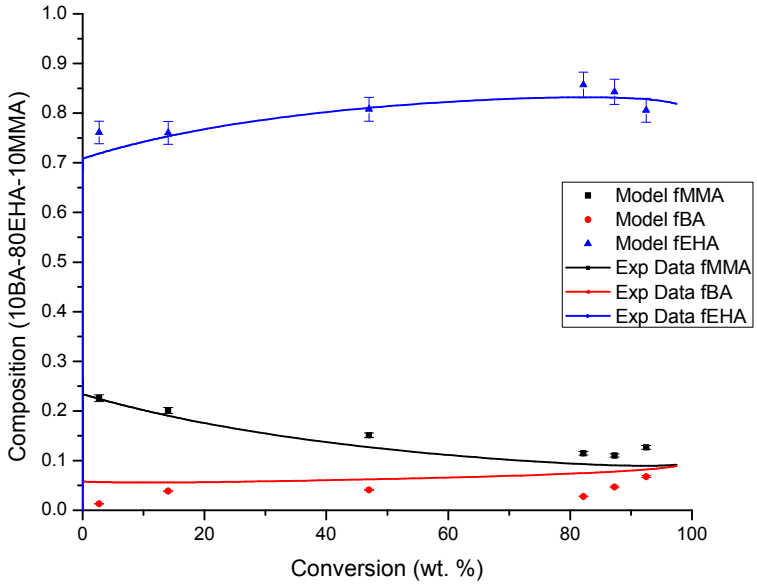

Figure 16. Comparison of experimental data and calculated profiles of copolymer composition for each monomer species versus conversion for a system with 10BA/80EHA/10MMA initial concentrations.

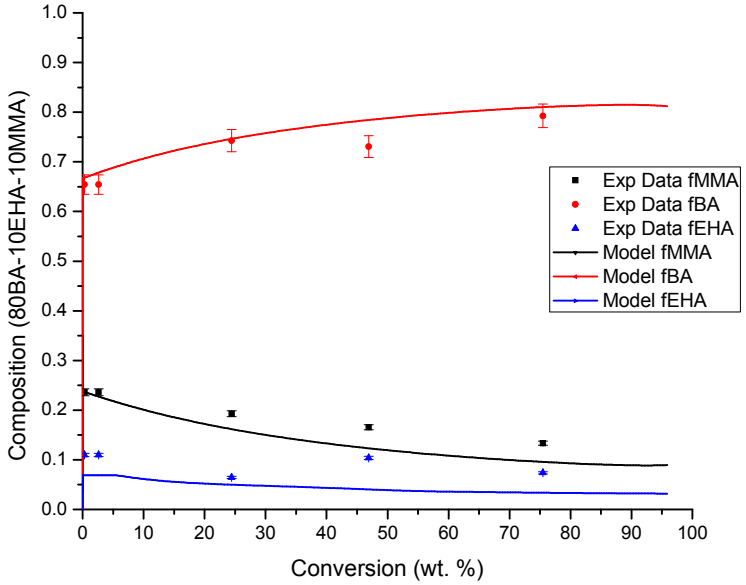

Figure 17. Comparison of experimental data and calculated profiles of copolymer composition for each monomer species versus conversion for a system with 80BA/10EHA/10MMA initial concentrations.

4.4. Molecular Weight versus Conversion Profiles

As observed in Figures 18–23, the agreement between experimental data and calculated profiles of molar mass (M_n, M_w and Đ) versus conversion for the copolymerizations of BA and EHA as well as MMA and EHA is reasonably good. Order of magnitude agreement was obtained in both cases. It is observed from the experimental data of M_n, M_w and Đ that changes on initial monomer composition do not have significant effects on the molecular weights and dispersity achieved. The same trend was predicted by the model at low conversions, but significant deviations are observed at high conversions (calculated M_w-and consequently Đ– being much higher than the corresponding experimental data).

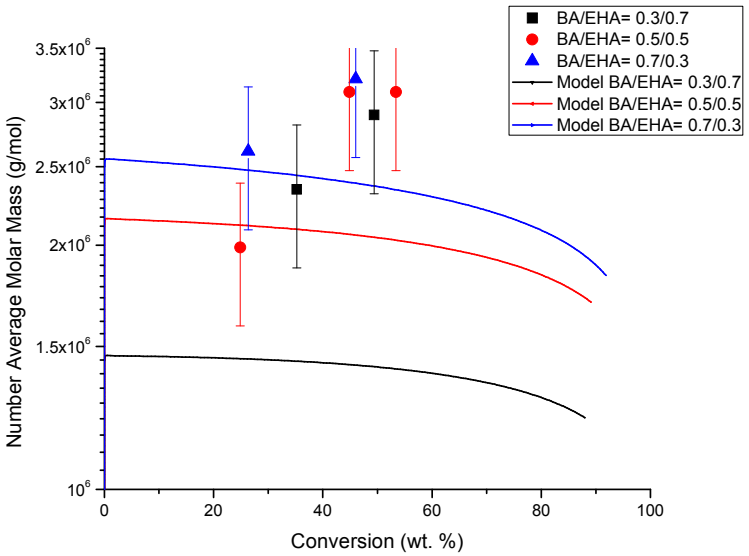

Figure 18. Comparison of experimental data and calculated profiles of number average molar mass versus conversion in the copolymerization of BA and EHA at different initial compositions of BA.

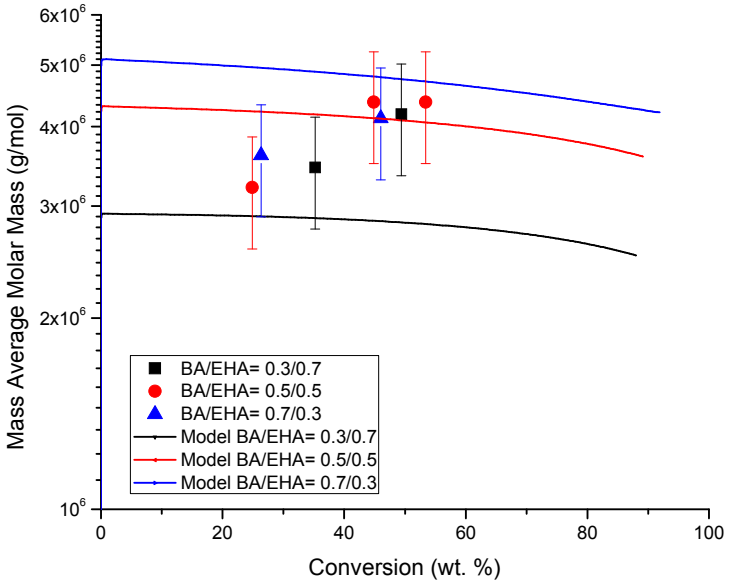

Figure 19. Comparison of experimental data and calculated profiles of weight average molar mass versus conversion in the copolymerization of BA and EHA at different initial compositions of BA.

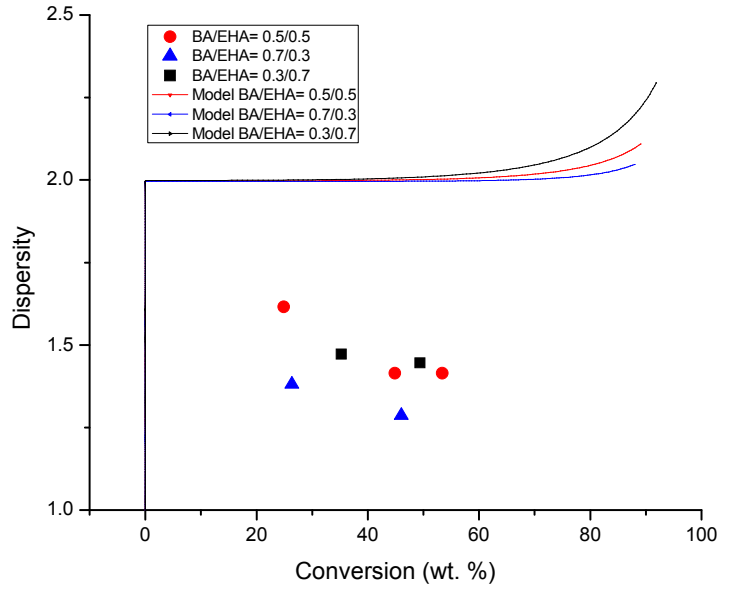

Figure 20. Comparison of experimental data and calculated profiles of Đ versus conversion in the copolymerization of BA and EHA at different initial compositions of BA.

As observed in Figures 21 and 22 for copolymerization of MMA and EHA, the model predicts a slightly faster increase of molar mass as the polymerization proceeds, namely, the calculated profiles of both M_n and M_w slightly overpredict the molar masses achieved. It is also observed in these figures that although the experimental profiles seem to overlap, the effect of increasing the amount of MMA in the initial monomer mixture is captured in the opposite direction by the model. The experimental profiles show that molecular weight increases as the amount of MMA is decreased, whereas the calculated profiles show the opposite trend. To solve this issue, a more complete experimental study for the homopolymerization of EHA would be useful, since the chain transfer to the EHA kinetic rate coefficient had to be estimated in this study. However, the increasing trend of molar mass as time elapses is nicely captured by the model. This increasing trend was possible to reproduce by including diffusion-controlled dependence to the chain transfer to monomer reaction. Otherwise, flat profiles were obtained.

In the case of copolymerization of BA and EHA, although order of magnitude predictions of M_n and M_w were obtained, which was partly possible by the inclusion of DC effects in the chain transfer to monomer and backbiting reactions; the evolution with conversion of the profiles was captured very poorly. This may be explained by the fact that crosslinking and gelation occurred in the experimental system and these phenomena were not included in the model. Furthermore, as noted in the original data reference [14], because the samples were filtered prior to analysis, only the soluble part of the polymer could be analyzed. This situation also explains the large discrepancy between experimental and calculated values of Đ observed in Figure 20.

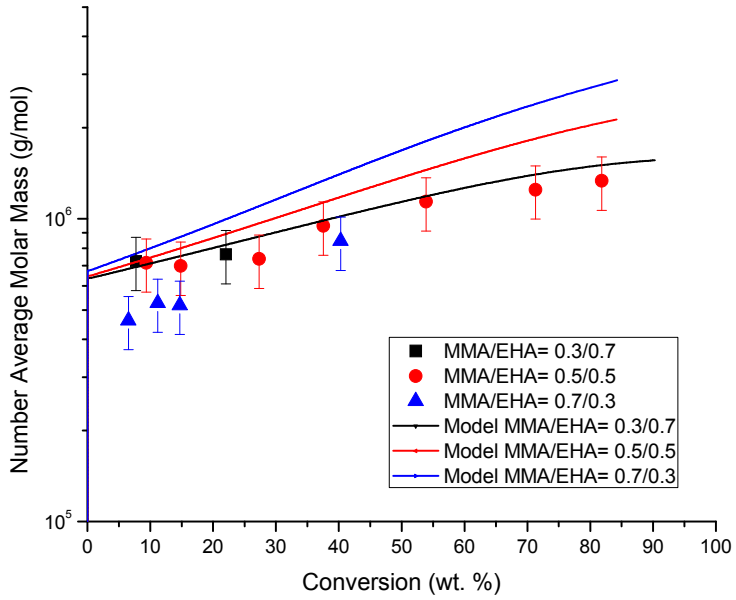

Figure 21. Comparison of experimental data and calculated profiles of number average molar mass versus conversion in the copolymerization of MMA and EHA at different initial compositions of MMA.

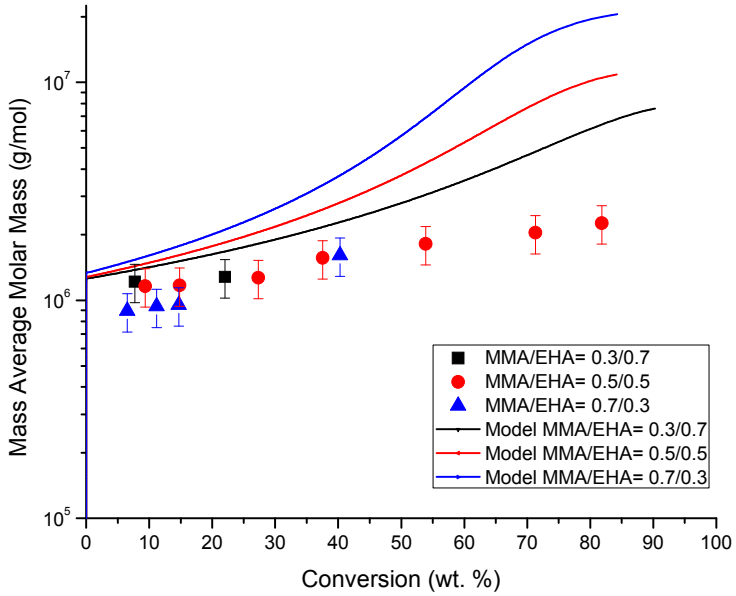

Figure 22. Comparison of experimental data and calculated profiles of weight average molar mas versus conversion in the copolymerization of MMA and EHA at different initial compositions of MMA.

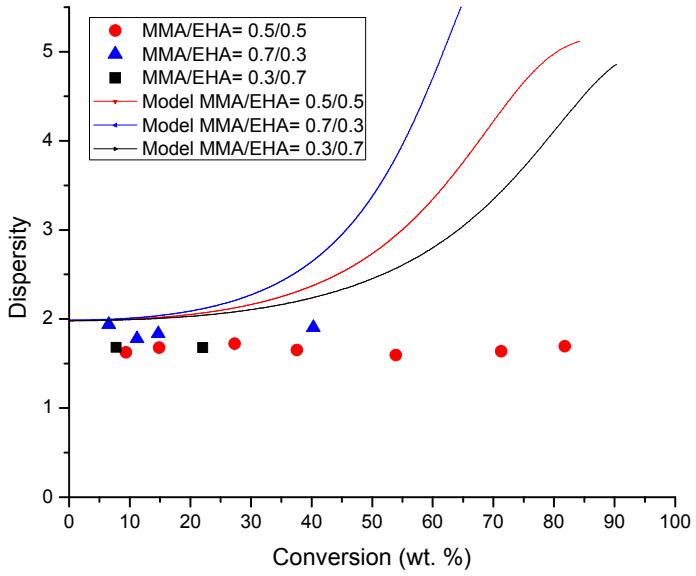

Figure 23. Comparison of experimental data and calculated profiles of Đ conversion in the copolymerization of MMA and EHA at different initial compositions of MMA.

It is observed in Figures 24 and 25 that our model is able to produce order-of-magnitude estimations of final molecular weights (M_n and M_w at high conversions), but their time (conversion) evolution is captured very poorly. As a matter of fact, the observed trends are opposite to the calculated profiles: The observed trend is that molecular weight increases within the same order of magnitude values, and the calculated profiles show huge decreasing trends (of about two orders of magnitude). Although this is not uncommon in polymerization modeling studies, these results may be attributed to the estimated k_{EHA} chain transfer to monomer kinetic rate constant coefficients. As stated in Section 3.8 of this contribution, k_{EHA} was used to fit BA/EHA and EHA/MMA copolymers molar masses. Since crosslinking and gelation occurred in the BA/EHA system, our estimation of k_{EHA} was likely overpredicted. More complete experimental studies with a focus on capturing the early stages of the polymerization and gathering more data on molecular weight development are needed to improve our model.

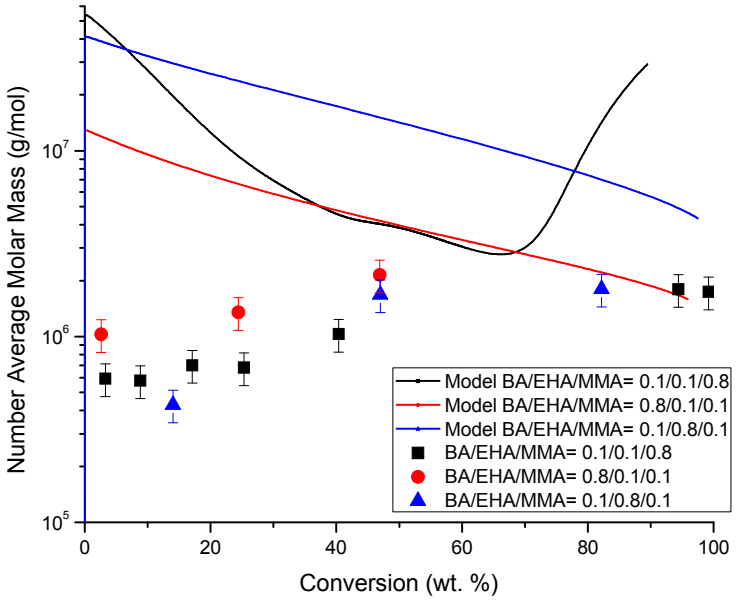

Figure 24. Comparison of experimental data and calculated profiles of number average molar mass versus conversion for terpolymerizations of BA, EHA and MMA at the initial concentrations indicated in the legend.

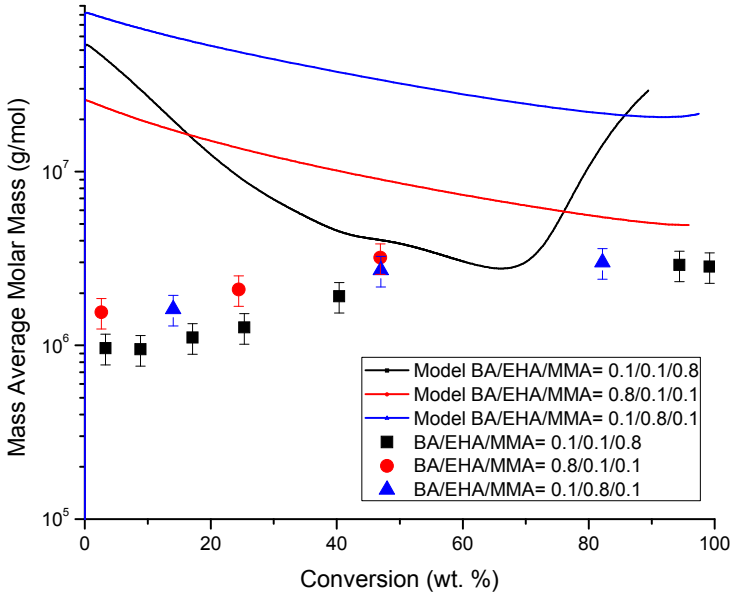

Figure 25. Comparison of experimental data and calculated profiles of weight average molar mass versus conversion for terpolymerizations of BA, EHA and MMA at the initial concentrations indicated in the legend.

5. Conclusions

MMA and BA are well-studied monomers whose polymerization kinetic rates coefficients are well known. However, this is not the case with EHA. Several important EHA kinetic rate coefficients (e.g., termination and transfer to monomer) had to be estimated in this study from experimental data not designed for such purposes.

The overall agreement between experimental data and model calculations for the three copolymerization systems was fairly good. Copolymer composition was captured very well with the model for systems BA/EHA and MMA/EHA. Some deviations between calculated and experimental data were observed in some cases for conversion versus time. Predictions of molecular weight development were rather poor in some cases, particularly for the terpolymer cases. Further experimental and modeling studies are needed, particularly for the estimation of chain transfer in EHA in bulk copolymerizations. From the experimental side, it would be useful to put more emphasis on reducing further or eliminating induction times (more through purification procedures) and gathering more experimental data for molecular weight development. Regarding the theoretical side, it would be useful to carry out simulations where BA is present with inclusion of crosslinking and gelation phenomena.

Finally, it is important to point out that our simulations were carried out using a global set of parameters. Namely, the parameters were not changed in individual cases to improve data fitting. If we had done that, our simulated profiles would have fit the experimental data much better, but that was not the point of our study.

Author Contributions: J.A.G.-R. performed all the simulations and parameter estimation procedure, guided by E.V.-L. M.A.D. and V.A.G. conceived the experimental research. V.A.G. conducted all experiments and characterization. M.A.D. and E.V.-L. provided technical direction to the project. J.A.G.-R. wrote the paper with feedback from V.A.G., while M.A.D. and E.V.-L. revised the final document.

Funding: This research was funded by: DGAPA-UNAM, grant numbers PAPIIT IG100718 and IV100119; Facultad de Química-UNAM, grant number PAIP 5000-9078.

Acknowledgments: Additional financial support from the following sources is gratefully acknowledged: (a) Consejo Nacional de Ciencia y Tecnología (CONACYT, México), MEng scholarship granted to J.A.G.-R.; and (b) Natural Sciences and Engineering Research Council (NSERC) of Canada.

Conflicts of Interest: The authors declare no conflict of interest.

Nomenclature

BA	n-Butyl Acrylate
EHA	2-Ethylhexyl Acrylate
MMA	Methyl Methacrylate
DC	Diffusion-Controlled (Effects)
PSA	Pressure Sensitive Adhesive
AIBN	Azobisisobutyronitrile
f_i	Monomer Fraction for species *i*
I	Initiator
I•	Primary Radical
M*i*	Monomer for species *i*
P*i*(s)•	Secondary Radical for species *i*
Q*i*(s)•	Tertiary Radical for species *i*
P*i*	Polymer for species *i*
P*i*(s)•	Secondary Radical for species *i*
ki	Initiator Decomposition Kinetic Rate Coefficient
f	Initiator Efficiency Factor
kp*i*	Propagation Kinetic Rate Coefficient for species *i*
kp*ij*	Cross-Propagation Kinetic Rate Coefficient for species *i*and *j*
kf*i*	Chain Transfer Kinetic Rate Coefficient for species *i*
kf*ij*	Cross-Chain Transfer Kinetic Rate Coefficient for species *i*
kbb	Backbiting Kinetic Rate Coefficient for n-Butyl Acrylate
kt*i*	Global Termination Kinetic Rate Coefficient for species *i*
ktc*i*	Termination by Combination Kinetic Rate Coefficient for species *i*
ktd*i*	Termination by Disproportionation Kinetic Rate Coefficient for species *i*
kf*i*tert	Tertiary Radical Chain Transfer Kinetic Rate Coefficient for species *i*
kp*i*tert	Tertiary Radical Propagation Kinetic Rate Coefficient for species *i*
ktc*ij*	Cross-Termination by Combination Kinetic Rate Coefficient for species *i*
ktd*ij*	Cross-Termination by Disproportionation Kinetic Rate Coefficient for species *i*
r*ij*	Reactivity Ratio beween species *i*and *j*
β	Attraction/Separation Overlap Factor in free-volume theory
α_M	Expansion Coefficient for Monomer
α_P	Expansion Coefficient for Polymer
v_f	Free Volume at a given calculated time
v_{fo}	Free volume at initial conditions
Vmi	Monomer Volume for species *i*
Vp*i*	Polymer Volume for species *i*
T_{gP}	Polymer Glass Temperature
T_{gM}	Monomer Glass Temperature
T	System Temperature

Appendix A

As stated in Section 3.8, the parameter estimation procedure consisted of a combination between careful literature review, detailed parameter sensitivity analyses and the use of educated guesses (trial and error guided from the information gained from the literature review and the parameter sensitivity analyses). The strategy is illustrated in this appendix with a few examples related to the estimation of kt_{EHA}, kf_{EHA} and the β-parameters for DC effects.

As shown in Figure A1 for system 30BA/70EHA, kt_{EHA} has a strong effect on polymerization rate and because of that it was used to fit conversion versus time data at low conversions (up to 20–30 wt. % monomer conversion). From the results shown in Figure A1, it seemed that $kt_{EHA} = 1 \times 10^8$ L mol^{-1} s^{-1} was the best fit. However, as shown in Figures A2 and A3 for systems 50BA/50EHA and 70BA/30EHA, respectively, that value was not the best for such systems. Therefore, the value of kt_{EHA} was set by using a single value ($kt_{EHA} = 5 \times 108$ L mol^{-1} s^{-1}) that could reproduce reasonably well the experimental data

for the three compositions and the experimental data (at different compositions) for system MMA/EHA (profiles not shown for those cases).

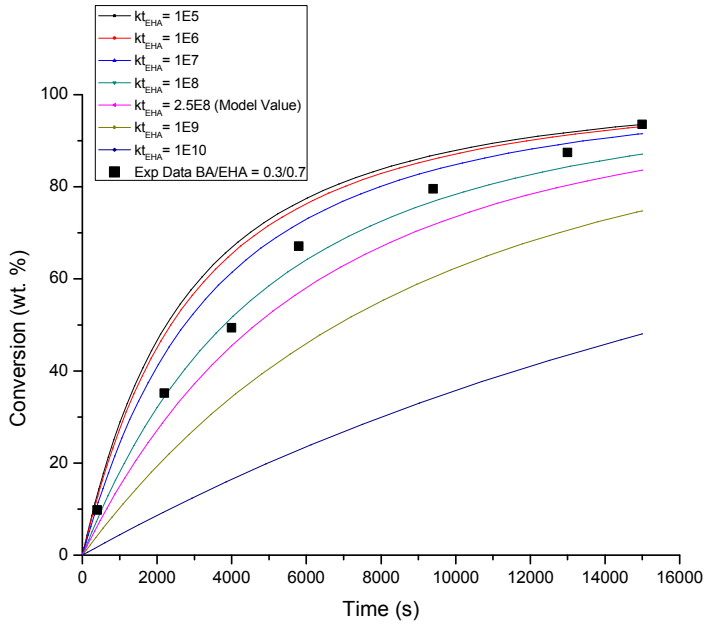

Figure A1. Effect of kt_{EHA} on conversion versus time profiles for system 30BA/70EHA.

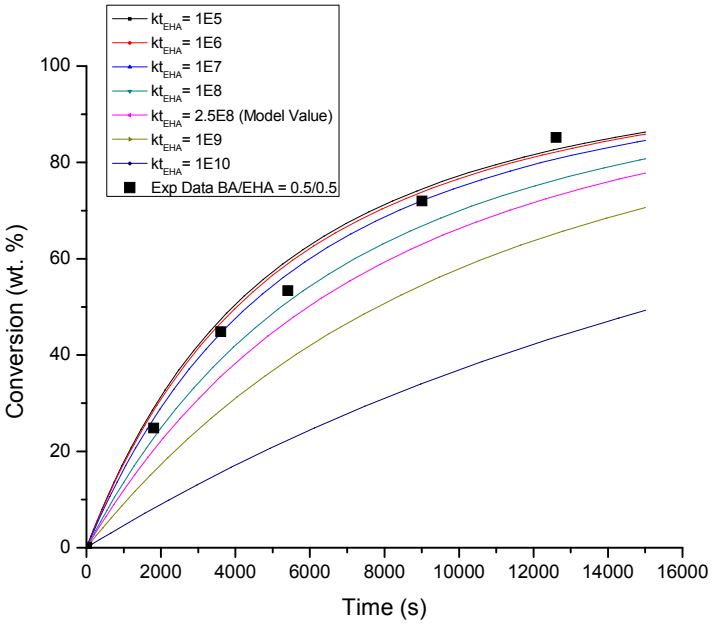

Figure A2. Effect of kt_{EHA} on conversion versus time profiles for system 50BA/50EHA.

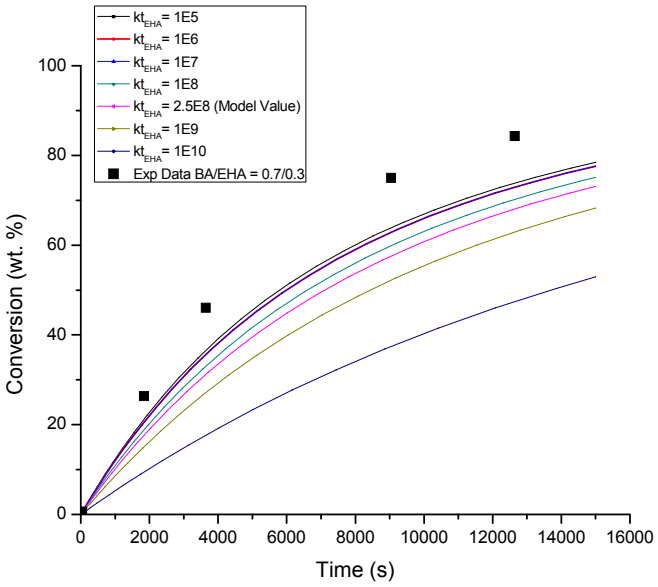

Figure A3. Effect of kt_{EHA} on conversion versus time profiles for system 70BA/30EHA.

The calculated conversion versus time profiles agreed well with experimental data at low conversions but deviated at the high conversion region. The agreement at high conversions was improved by considering DC effects, namely, by adjusting βp and βt. When carrying out parameter sensitivity analyses for those parameters, it was found that it was the ratio of them, which was useful for data fitting purposes. Table A1 and Figures A4–A6 show some of the data sets used for estimation of βp and βt (Table A1 and Section 3.7) and the profiles obtained for the BA/EHA system. As shown in Figure A7 DC effects also affect the composition versus conversion profiles, a fact that was also considered in the estimation of the DC β-parameters.

Table A1. Tested β_t/β_p ratios for BA/EHA system.

	BA β_t/β_p	EHA β_t/β_p	BA/EHA β_t/β_p	Figure
Set 1	32	16	4	A4
Set 2 (Model)	16	8	2	A5 (2)
Set 3	8	4	1	A6

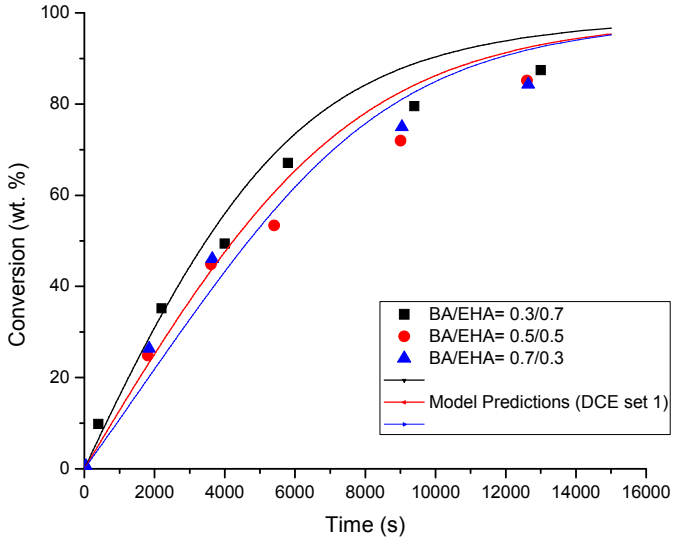

Figure A4. Effect of the ratio β_t/β_p (DC effects) on conversion versus time profiles for system BA/EHA (Set 1 of Table A1).

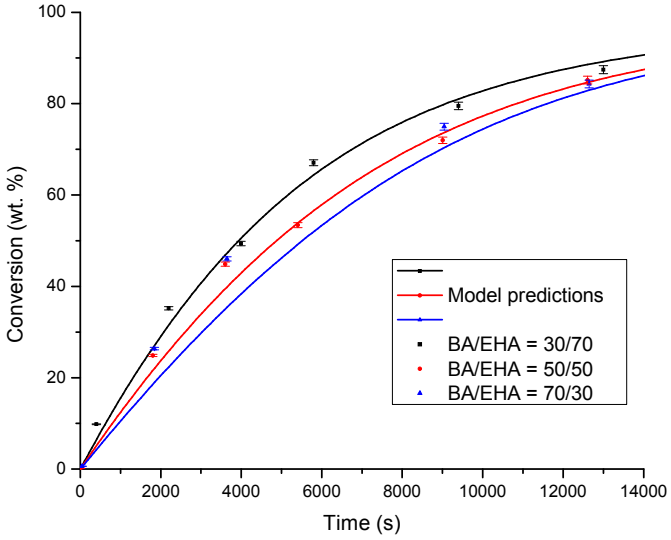

Figure A5. (Figure 2) Effect of the ratio β_t/β_p (DC effects) on conversion versus time profiles for system BA/EHA (Set 2 of Table A1).

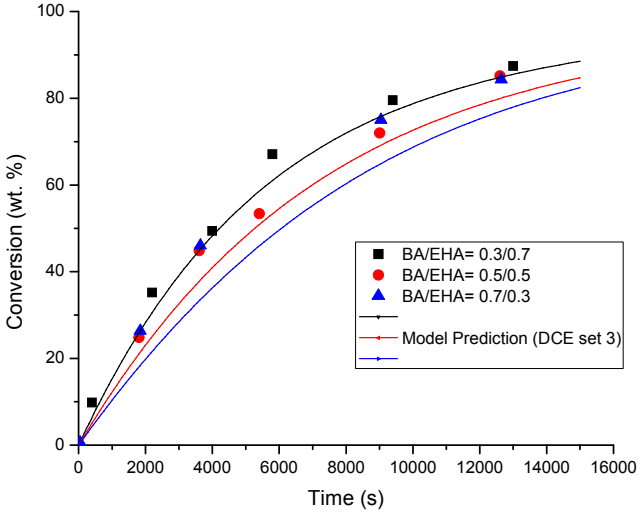

Figure A6. Effect of the ratio β_t/β_p (DC effects) on conversion versus time profiles for system BA/EHA (Set 3 of Table A1).

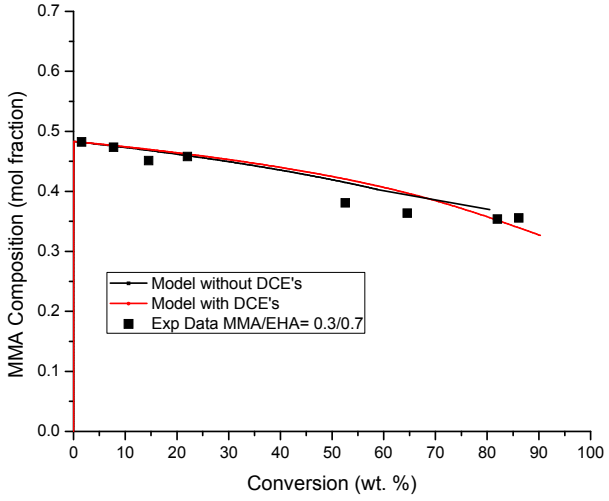

Figure A7. Comparison of modeling profiles of copolymer composition (MMA content) versus conversion, considering or neglecting DC effects, for system 30MMA/70EHA.

It is common knowledge in free radical polymerization that chain transfer reactions to small molecules may significantly affect molar mass development without affecting polymerization rate. This was the case for chain transfer to EHA. As observed in Figure A8, changing kf_{EHA} by three orders of magnitude resulted on minimal effect on polymerization rate, but significant changes on molecular weight development (see Figure A9).

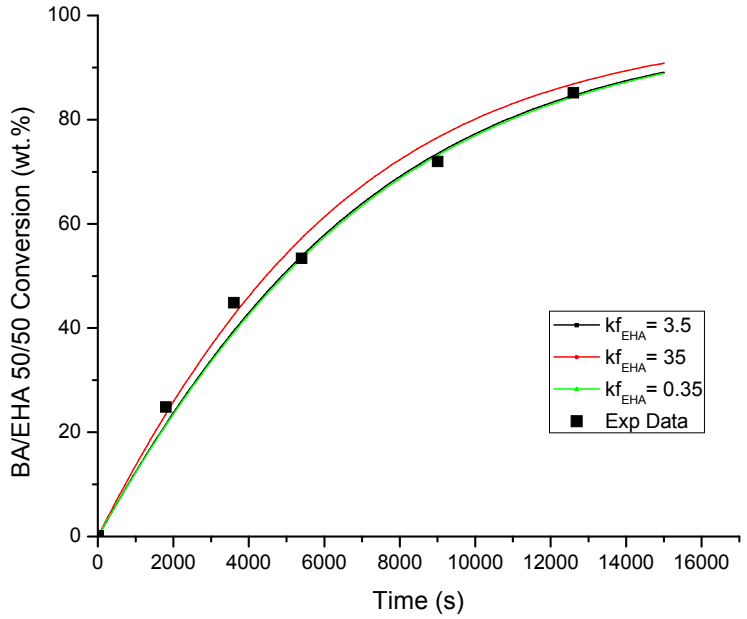

Figure A8. Effect of kf_{EHA} on conversion versus time profiles for system 50BA/50EHA.

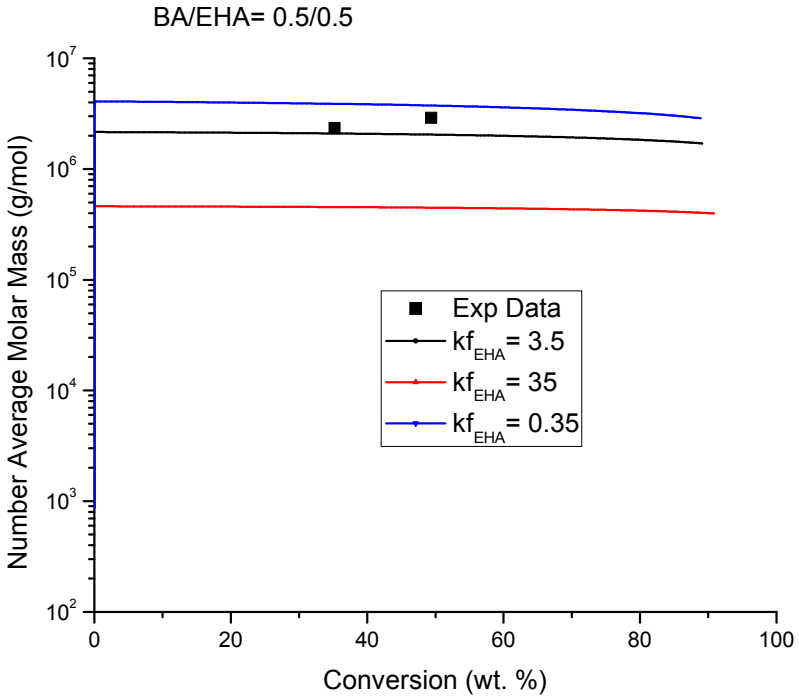

Figure A9. Effect of kf_{EHA} on M_n versus conversion profiles for system 50BA/50EHA.

kf_{EHA} was therefore used to fit molecular weight development data for the studied systems. As observed in Figures A10–A12, the best agreement with experimental data of M_n versus conversion was obtained with kf_{EHA} = 2 L mol^{-1} s^{-1}, but the best agreement with experimental data of M_w versus conversion was obtained with kf_{EHA} = 5 L mol^{-}1 s^{-1} (see Figures A13–A15). A compromise

was established by using a final value of kf_{EHA} = 3.5 L mol^{-1} s^{-1}. As explained in the body of the manuscript, gelation was an issue for systems containing BA, so that explains the deviation. Chain transfer to tertiary radicals for EHA was adjusted similarly, but its effect on molar mass development had less impact on molar mass results.

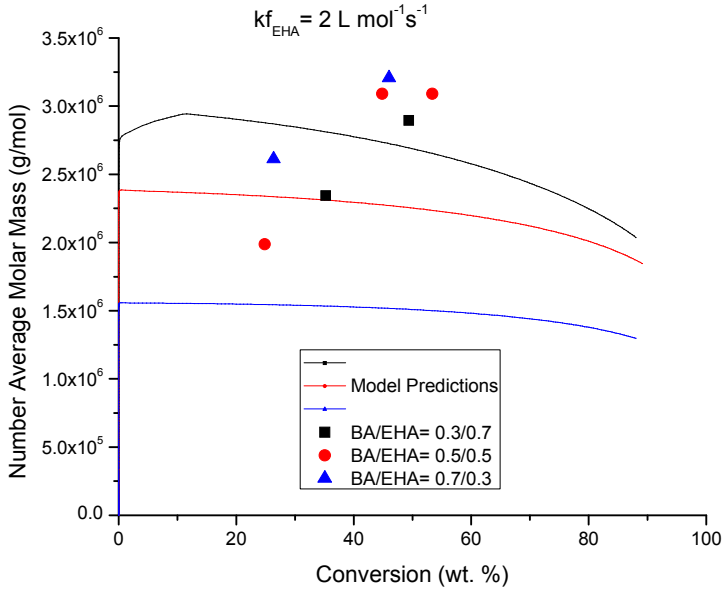

Figure A10. Comparison of experimental and calculated profiles of M_n versus conversion for system BA/EHA using kfEHA = 2 L mol^{-1} s^{-1}.

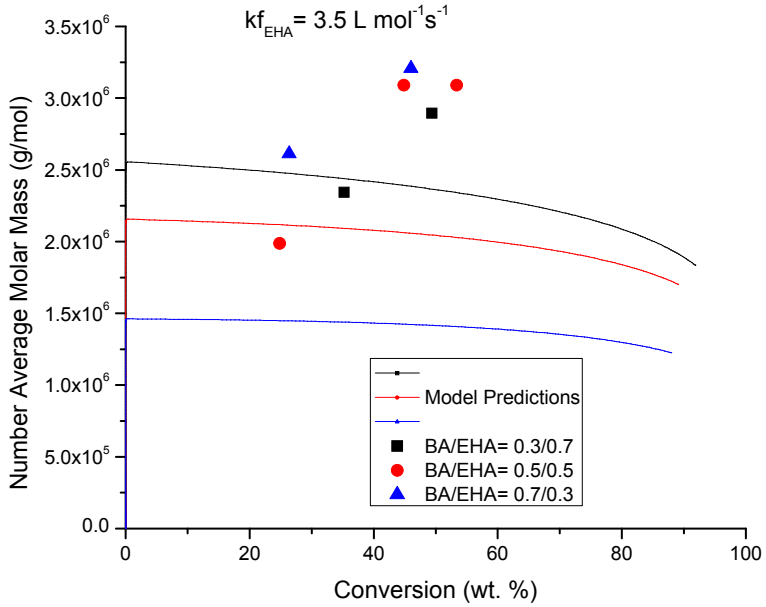

Figure A11. Comparison of experimental and calculated profiles of M_n versus conversion for system BA/EHA using kfEHA = 3.5 L mol^{-1} s^{-1}.

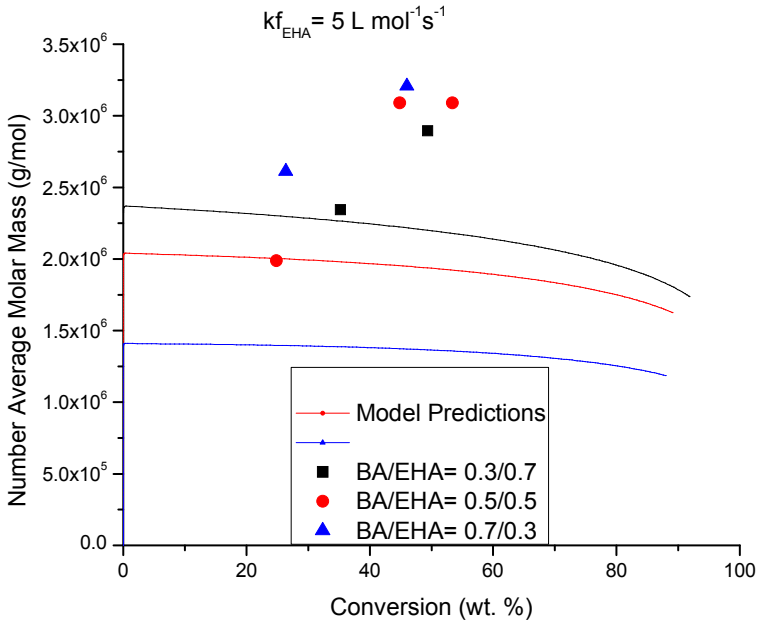

Figure A12. Comparison of experimental and calculated profiles of M_n versus conversion for system BA/EHA using kfEHA = 5 L mol^{-1} s^{-1}.

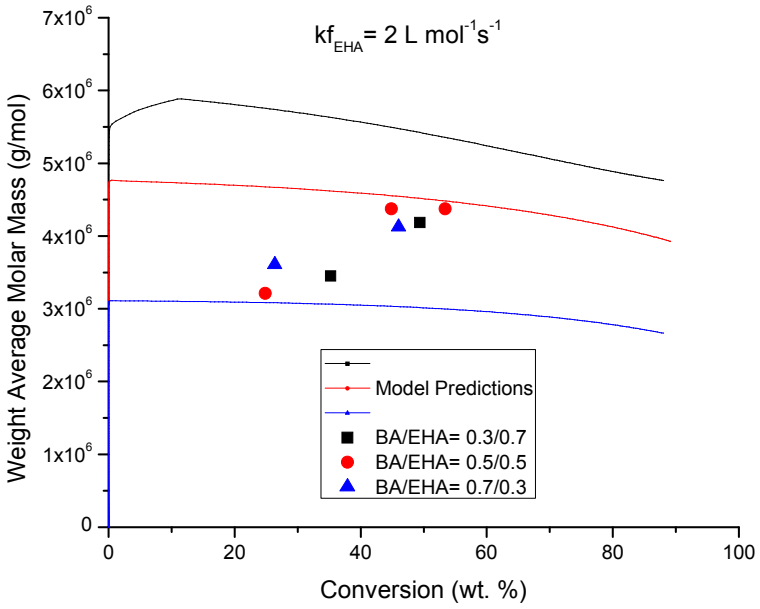

Figure A13. Comparison of experimental and calculated profiles of M_w versus conversion for system BA/EHA using kfEHA = 2 L mol^{-1} s^{-1}.

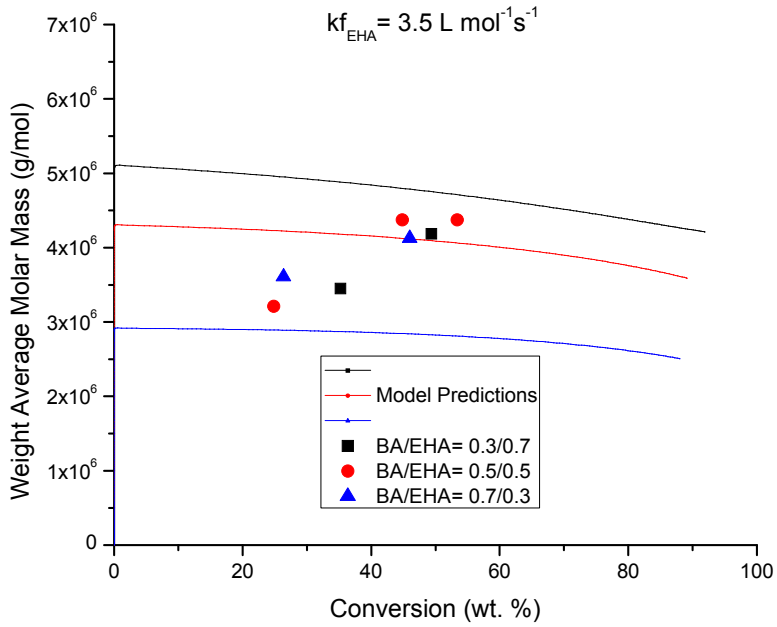

Figure A14. Comparison of experimental and calculated profiles of M_w versus conversion for system BA/EHA using kfEHA = 3.5 L mol^{-1} s^{-1}.

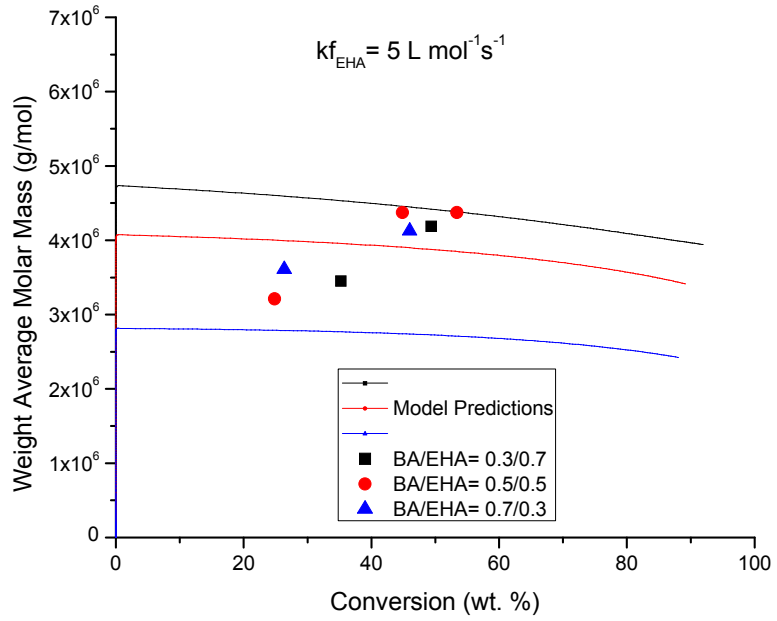

Figure A15. Comparison of experimental and calculated profiles of M_w versus conversion for system BA/EHA using kfEHA = 5 L mol^{-1} s^{-1}.

References

1. Dubé, A.M.; Zapata-González, I. Ch. 6: Copolymerization. In *Handbook of Polymer Synthesis, Characterization, and Processing*; Saldívar-Guerra, E., Vivaldo-Lima, E., Eds.; John Wiley & Sons: Hoboken, NJ, USA, 2013; pp. 105–125.
2. Learner, T.J.S.; Krueger, J.W.; Schilling, M.R. Modern Paints Uncovered. In Proceedings of the Modern Paints Uncovered Symposium, London, UK, 16–19 May 2006; Learner, J.S., Smithen, P., Krueger, J.W., Schilling, M.R., Eds.; Getty Conservation Institute: London, UK, 2007.
3. Moghbeli, M.R.; Zamir, S.M.; Molaee, B. Resultant Synergism in the Shear Resistance of AcrylicPressure-Sensitive Adhesives Prepared by EmulsionPolymerization of n-Butyl Acrylate/2-Ethyl HexylAcrylate/Acrylic Acid. *J. Appl. Polym. Sci.* **2008**, *108*, 606–613. [CrossRef]

4. Srivastava, S. Co-polymerization of Acrylates. *Des. Monomers Polym.* **2009**, *12*, 1–18. [CrossRef]
5. Benedek, I. *Pressure-Sensitive Adhesives and Applications*, 2nd ed.; Springer-Verlag: Leipzig, Germany, 2004; pp. 5–10.
6. Gao, J.; Penlidis, A. A Comprehensive Simulator Database Package for Reviewing Free-Radical Copolymerizations. *Macromol. React. Eng.* **1998**, *38*, 651–780. [CrossRef]
7. Beuermann, S.; Paquet, D.A.; McMinn, J.H.; Hutchinson, R.A. Determination of Free-Radical Propoagation Rate Coefficients of Butyl, 2-Ethylhexyl, and Dodecyl Acrylates by Pulsed-Laser Polymerization. *Macromolecules* **1996**, *29*, 4206–4215. [CrossRef]
8. Agirre, A.; Nase, J.; Degrandi, E.; Creton, C.; Asua, J.M. MiniemulsionPolymerization of 2-Ethylhexyl Acrylate. Polymer Architecture Control and Adhesion Properties. *Macromolecules* **2010**, *43*, 8924–8932. [CrossRef]
9. Capek, I.; Juranicova, V.; Barton, J.; Asua, J.M.; Ito, K. Microemulsion Radical Polymerization ofAlkyl Acrylates. *Polym. Int.* **1997**, *43*, 1–7. [CrossRef]
10. Plessis, C.; Arzamendi, G.; Alberdi, J.M.; Agnely, M.; Leiza, J.R.; Asua, J.M. Intramolecular Chain Transfer to Polymer in the Emulsion Polymerization of 2-EthylhexylAcrylate. *Macromolecules* **2001**, *34*, 6138–6143. [CrossRef]
11. Heatley, F.; Lovell, P.A.; Yamashita, T. Chain Transfer to Polymer in Free-Radical Solution Polymerization of2-Ethylhexyl Acrylate Studied by NMR Spectroscopy. *Macromolecules* **2001**, *34*, 7636–7641. [CrossRef]
12. Couvreur, L.; Piteau, G.; Castignolles, P.; Tonge, M.; Coutin, B.; Charleux, B.; Vairon, J.P. Pulsed-Laser Radical Polymerization and Propagation Kinetic Parameters of Some Alkyl Acrylates. *Macromol. Symp.* **2001**, *174*, 197–207. [CrossRef]
13. Junkers, T.; Schneider-Baumann, M.; Koo, S.S.; Castignolles, P.; Barner-Kowollik, C. Determination of propagation rate coefficients for methyl and 2-ethylhexyl acrylate via high frequency PLP-SEC under consideration of the impact of chain branching. *Macromolecules* **2010**, *43*, 10427–10434. [CrossRef]
14. Gabriel, V.A.; Dubé, M.A. Bulk Free-Radical Co- and Terpolymerization of n-Butyl Acrylate/2-Ehylhexyl Acrylate/MethylMethacrylate. *Macromol. React. Eng.* **2018**. [CrossRef]
15. Bicak, N.; Ozlem, M. Graft Copolymerization of Butyl Acrylate and 2-Ethyl HexylAcrylate from Labile Chlorines of Poly(vinyl chloride) byAtom Transfer Radical Polymerization. *J. Polym. Sci.* **2003**, *41*, 3457–3462. [CrossRef]
16. Percec, V.; Popov, A.V.; Ramirez-Castillo, E.; Hinojosa-Falcon, L.A. Synthesis of Poly(vinyl chloride)-b-Poly(2-ethylhexylacrylate)-b-Poly(vinyl chloride) by the Competitive Single-Electron-Transfer/Degenerative-Chain-Transfer MediatedLiving Radical Polymerization of Vinyl Chloride Initiatedfromα,ω-Di(iodo)poly(2-ethylhexyl acrylate) and Catalyzedwith Sodium Dithionite in Water. *J. Polym. Sci.* **2005**, *43*, 2276–2280.
17. Vidts, K.R.M.; Dervaux, B.; Prez, F.E.D. Block, Blocky Gradient and Random Copolymers of 2-Ethylhexyl Acrylate and Acrylic Acid by Atom Transfer Radical Polymerization. *Polymer* **2006**, *47*, 6028–6037. [CrossRef]
18. Haloi, D.J.; Singha, N.K. Synthesis of Poly(2-ethylhexyl acrylate)/Clay Nanocompositeby In Situ Living Radical Polymerization. *J. Polym. Sci.* **2011**, *49*, 1564–1571. [CrossRef]
19. Achilias, D.S. Review of Modeling of Diffusion Controlled Polymerization Reactions. *Macromol. Theory Simul.* **2007**, *16*, 319–347. [CrossRef]
20. Buback, M.; Huckestein, B.; Russell, G.T. Modeling of termination in intermediate and high conversion free radical polymerizations. *Macromol. Chem. Phys.* **1994**, *195*, 539–554. [CrossRef]
21. Stickler, M.; Panke, D.; Hamielec, A.E. Polymerization of Methyl Methacrylate up to High Degrees of Conversion: Experimental Investigation of the Diffusion-controlled Polymerization. *J. Polym. Sci. Polym. Chem.* **1984**, *22*, 2243–2253. [CrossRef]
22. Arzamendi, G.; Plessis, C.; Leiza, J.R.; Azua, J.M. Effect of the Intramolecular Chain Transfer to Polymer on PLP/SEC Experiments of Alkyl Acrylates. *Macromol. Theory Simul.* **2003**, *12*, 315–324. [CrossRef]
23. Lena, J.B.; Deschamps, M.; Sciortino, N.F.; Masters, S.L.; Squire, M.A.; Russell, G.T. Effects of Chain Transfer Agent and Temperature on Banching and β-Scission in Radical Polymerization of 2-Ethylhexyl Acrylate. *Macromol. Chem. Phys.* **2018**, *219*, 1700579. [CrossRef]
24. Plessis, C.; Arzamendi, G.; Alberdi, J.M. Evidence of Branching in Poly(butyl acrylate) Produced in Pulsed Laser Polymerization Experiments. *Macromol. Rapid Commun.* **2003**, *24*, 173–177. [CrossRef]
25. Ren, S.; Vivaldo-Lima, E.; Dubé, M.A. Modeling of the Copolymerization Kinetics of n-Butyl Acrylate and D-Limonene Using PREDICI. *Processes* **2015**, *4*, 1. [CrossRef]

26. Zhu, S.; Hamielec, A.E. Heat effects for free-radical polymerization in glass ampoules reactors. *Polymer* **1991**, *32*, 3021–3025. [CrossRef]
27. Zoller, A.; Gigmes, D.; Guillaneuf, Y. Simulation of radical polymerization of methyl methacylate at room temperaturre using a tertiary amine/BPO initiating system. *Polym. Chem.* **2015**, *6*, 1–3. [CrossRef]
28. Wulkow, M. Computeir Aided Modeling of Polymer Reaction Engineering-The Status of Predici, 1-Simulation. *Macromol. React. Eng.* **2008**, *2*, 461–494. [CrossRef]
29. Peikert, P.; Pflug, K.M.; Busch, M. Modeling of High-Pressure Ethene Homo- and Copolymerization. *Chem. Ing. Tech.* **2019**, *91*, 1–6.
30. Louie, B.M.; Carratt, G.M.; Soong, D.S. Modeling the free radical solution and bulk polymerization of methyl methacrylate. *J. Appl. Polym. Sci.* **1985**, *30*, 3985–4012. [CrossRef]
31. Penlidis, A. *Watpoly Database*; University of Waterloo: Waterloo, ON, Canada, 1992.
32. Rantow, E.S.; Soroush, M.; Grady, M.C.; Kalfas, G.A. Spontaneous polymerization and chain microstructure evolution in high-temperature solution polymerization of n-butyl acrylate. *Polymer* **2006**, *47*, 1423–1435. [CrossRef]
33. Dorschner, D. Multicomponent Free Radical Polymerization Model Refinements and Extensions with Depropagations. Master's Thesis, University of Waterloo, Department of Chemical Engineering, Waterloo, ON, Canada, 2010.
34. McManus, N.T.; Dubé, M.A. PeNLIDIS. *Polym. React. Eng.* **1999**, *7*, 131. [CrossRef]
35. Hungenberg, K.D.; Wulkow, M. *Modeling and Simulation in Polymer Reaction Engineering (A Modular Approach)*; Wiley-VCH: Weinheim, Germany, 2018; pp. 92–256.
36. Scott, A.J.; Penlidis, A. Ready-to-Use Computattional Package for Copolymerzation Reactivity Ratio Estimation: Improved Acces to the Error-in-Variables-Model. *Process* **2017**, *5*, 1–41.
37. Peck, A.N.F.; Hutchinson, R.A. Secondaryreactions in thehigh-temperature free radical polymerizationofbutyl acrylate. *Macromolecules* **2004**, *37*, 5944–5951. [CrossRef]
38. Ahmad, N.M.; Heatley, F.; Lovell, P.A. Chain Transfer Copolymer in Free-radical Solution Polymerizationof n-Butyl Acrylatestudiedby NMR spectroscopy. *Macromolecules* **1998**, *31*, 2822–2827. [CrossRef]
39. Theis, A.; Feldermann, A.; Charton, N.; Davies, T.P.; Stenzel, M.H.; Kowollik, C.B. Living free radical polymerization (RAFT) of dodecyl acrylate: Chain length dependent termination, mid-chain radicals and monomer reaction order. *Polymer.* **2005**, *46*, 6797–6809. [CrossRef]
40. Hamielec, A.E. Recent Developments in Free Radical Polymerization at High Conversion Diffusion Controlled Termination and Propagation. *Chem. Eng. Commun.* **1983**, *24*, 1–19. [CrossRef]
41. D'hooge, R.D.; Reyniers, M.F.; Marin, G.B. The Crucial Roles of Diffusional Limitantion in Controlled Radical Polymerization. *Macromol. React. Eng.* **2013**, *7*, 362–379.